

Tiago de Freitas Pereira

A COMPARATIVE STUDY OF COUNTERMEASURES TO DETECT SPOOFING ATTACKS IN
FACE AUTHENTICATION SYSTEMS

Campinas
2013

Universidade Estadual de Campinas
Faculdade de Engenharia Elétrica e de Computação

Tiago de Freitas Pereira

A COMPARATIVE STUDY OF COUNTERMEASURES TO DETECT SPOOFING ATTACKS IN
FACE AUTHENTICATION SYSTEMS

Qualificação de Mestrado apresentada na Faculdade de Engenharia Elétrica e de Computação como parte dos requisitos exigidos para a obtenção do título de Mestre em Engenharia Elétrica. Área de concentração: Computação

Orientador: Professor Doutor José Mario De Martino

Este exemplar corresponde a versão final do exame de qualificação apresentado pelo aluno, e orientado pelo Prof. Dr. José Mario De Martino

Campinas
2013

FAÇA AQUI SUA DEDICATÓRIA.

Acknowledgment

Text

A maravilhosa disposição e harmonia do universo só pode ter tido origem segundo o plano de um Ser que tudo sabe e tudo pode. Isto fica sendo a minha última e mais elevada descoberta.

Isaac Newton

Abstract

User authentication is an important step to protect information and in this field face biometrics is advantageous. Face biometrics is natural, easy to use and less human-invasive. Unfortunately, recent work has revealed that face biometrics is vulnerable to spoofing attacks using low-tech equipments. Countermeasures have been proposed in order to mitigate this vulnerabilities. However several works in the literature present evaluations using different metrics and in private database making the comparison of countermeasures a difficult task. The main goal of this masters project is to provide a comparative study of countermeasures against face *spoofing* attacks.

Key-words: Antispoofing, Liveness detection, Countermeasure, Face Recognition, Biometrics

List of Figures

2.1	5
3.1	Creating a fake fingerprint	7
3.2	Biometric data flow in a face authentication system	9
3.3	New google face unlock screen	10
3.4	Selection of face regions	11
3.5	Block diagram of the countermeasure based on LBP	12
3.6	Block diagram of the DoG countermeasure	13
3.7	Printed photo attacks of the NUAA database	14
3.8	Some frames of real access and spoofing attempts	15
3.9	Example images of real accesses and the corresponding spoofing attempts	17
4.1	(a) Three planes intersecting one pixel (b) LBP histogram of each plane (c) Concatenating the histograms).	20
4.2	Example sequence of a warped photo attack from the CASIA Face Anti-Spoofing Database ZHANG describing the characteristic reflections (flickering) of planar spoofing medium and the distorted motion patterns.....	21
4.3	Block diagram of the proposed countermeasure.	22
4.4	Face detection strategy for $R_t = 1$	22
4.5	(Color online) Evaluation of HTER(%) in each plane when the multiresolution area (R_t) is increased with LBP-TOP $_{8,8,8,1,1,R_t}^{u2}$ and LDA classifier - test-set (a) Replay-Attack Database (b) CASIA Face Anti-Spoofing Database.	24
4.6	(Color online) Evaluation of HTER(%) with LBP-TOP $_{8,8,8,1,1,R_t}^{u2}$ using different classifiers (a) Replay-Attack Database (b) CASIA Face Anti-Spoofing Database.	26
4.7	(Color online) Evaluation of HTER(%) with LBP-TOP $_{8,8,8,1,1,R_t}^{u2}$ using different LBP configurations in the planes with SVM classifier (a) Replay-Attack Database (b) CASIA Face Anti-Spoofing Database.	27
4.8	(Color online) Evaluation of the histogram size when (R_t) is increased.	27
4.9	(Color online) Evaluatation of HTER% using LBP-TOP $_{8,8,8,1,1,R_t}^{u2}$ with the single resolution and the multiresolution approach using SVM classifier (a) Replay-Attack Database (b) CASIA Face Anti-Spoofing Database.	28

4.10 (Color online) Access attempt based evaluation of different time window sizes using mean of features and mean of scores with LBP-TOP _{8,8,8,1,1,1} ^{u2} (a) Replay-Attack Database (HTER %) (b) CASIA Face Anti-Spoofing Database (EER %).	29
4.11 (Color online) Overall performance of LBP-TOP _{8,8,8,1,1,1} ^{u2} using average of features compared to the DoG baseline method and LBP _{8,1} ^{u2} on the CASIA Face Anti-Spoofing Database.	30
4.12 (Color online) Performance of LBP-TOP _{8,8,8,1,1,1} ^{u2} using average of features compared to the DoG baseline method and LBP _{8,1} ^{u2} under the different protocols of the CASIA Face Anti-Spoofing Database.	31
6.1 ROC curves of each countermeasure using the intra-test and the inter-test protocol. (a) Correlation with frame differences countermeasure trained and tuned with the Replay Attack Database (b) <i>LBP – TOP</i> countermeasure trained and tuned with the Replay Attack Database (c) <i>LBP</i> countermeasure trained and tuned with the Replay Attack Database (d) Correlation with frame differences countermeasure trained and tuned with the CASIA-FASD (e) <i>LBP – TOP</i> countermeasure trained and tuned with the CASIA-FASD (f) <i>LBP</i> countermeasure trained and tuned with the CASIA-FASD.	39
6.2 ROC curves of each countermeasure trained with Replay Attack Database and CASIA FASD and test it with each test set of each database. (a) Correlation with frame differences (b) <i>LBP – TOP</i> countermeasure (c) <i>LBP</i> countermeasure	40
6.3 ROC curves of each countermeasure trained with the Score Level Fusion based Framework (a) Correlation with frame differences (b) <i>LBP – TOP</i> countermeasure (c) <i>LBP</i> countermeasure.	41

List of Tables

2.1	Comparison of the most used biometric traits	4
3.1	Performance in <i>HTER</i> (%) terms of the LBP countermeasure in three face spoofing databases.	13
3.2	Number of videos in each subset. Numbers displayed as sums indicate the amount of hand-based and fixed support attack available in each subset.	16
4.1	EER (in %) comparison between the DoG baseline method, $LBP_{8,1}^{u2}$ and $LBP-TOP_{8,8,8,1,1,1}^{u2}$ using average of features on the CASIA Face Anti-Spoofing Database.	30
4.2	EER (in %) development of $LBP-TOP_{8,8,8,1,1,1}^{u2}$ using average of features on the CASIA Face Anti-Spoofing Database.	32
4.3	<i>HTER</i> (%) of the best results achieved on the Replay-Attack Database (following the database protocol) comparing with the provided baseline.	32
4.4	<i>EER</i> (%) of the best results achieved on the CASIA Face Anti-Spoofing Database (following the database protocol) comparing with the provided baseline.	33
6.1	<i>HTER</i> (%) of each countermeasure applying the intra-test ($D_1 = D_2$) protocol. .	38
6.2	<i>HTER</i> (%) of each countermeasure applying the inter-test ($D_1 \neq D_2$) protocol. .	38
6.3	<i>HTER</i> (%) of each countermeasure trained with Replay Attack Database and CASIA FASD and test it with each test set of each database.	40
6.4	Q -statistic and <i>HTER</i> (%) of each countermeasure trained with the Score Level Fusion based Framework and test it with each database.	41

Acronyms

Contents

1	Introduction	1
1.1	Scope and Contributions	1
1.2	Organization of the Thesis	1
2	Biometrics	3
2.1	Introduction to Biometric Systems	3
2.2	Attacks in Biometric Systems	4
2.2.1	Replay attack	4
2.2.2	Biometric reference attack	5
2.2.3	Man-in-the-middle	5
2.2.4	Ataque de Spoofing	6
2.3	Final Remarks	6
3	Spoofing Attacks	7
3.1	Spoofing Attacks in Biometrics	7
3.1.1	Fingerprint	7
3.1.2	Speaker	8
3.1.3	Iris	8
3.2	Spoofing Attacks in Face Recognition	8
3.2.1	Presence of vitality (liveness detection)	10
3.2.2	Scene	11
3.2.3	Differences in image quality assessment	12
3.3	Face Spoofing Databases	14
3.3.1	NUAA	14
3.3.2	Replay-Attack Database	15
3.3.3	CASIA Face Anti-Spoofing Database	16
3.4	Final Remarks	17
4	Developed Countermeasures	19
4.1	LBP based dynamic texture description	19
4.2	Architecture of the countermeasure	22

4.3	Experiments	23
4.3.1	Effectiveness of each <i>LBP – TOP</i> plane individually and in combination	24
4.3.2	Effectiveness of different classifiers	25
4.3.3	Effectiveness of different LBP operators	25
4.3.4	Effectiveness of the multiresolution approach	26
4.3.5	Access attempt based analysis	28
4.3.6	Summary	31
4.4	Final Remarks	32
5	The Comparative Study	35
5.1	Databases Permeability	35
5.2	Evaluation Protocol	35
5.2.1	Intra Database Test Protocol	35
5.2.2	Inter Database Test Protocol	35
5.2.3	Evaluation Metrics	36
6	Experiments and Results	37
6.1	Intra-test protocol	37
6.2	Inter-test protocol	38
6.3	Combination of Multiple Databases	39
6.4	Score Level Fusion based Framework	39
7	Conclusion	43
8	Future Work	45
A	Related Publications	47
References		48

Introduction

1.1 Scope and Contributions

1.2 Organization of the Thesis

Chapter 2

Biometrics

This chapter presents the concepts related to Biometrics and the security issues related. Section 2.1 presents what is a biometric authentication system. Section 2.2 presents the main threats in a biometric authentication system. Finally, Section 2.3 presents the Final Remarks of the chapter.

2.1 Introduction to Biometric Systems

Biometrics is the science of recognizing the identity of a person based on their physical attributes and / or behavior, such as face, fingerprints, hand veins, voice or iris (Li & Jain 2011). The use of biometrics as authentication factor has some advantages. Naturally, is not possible to forget or transfer a biometric trait and it hardly disappears (perhaps in case of a seriously accidents). Biometrics has some drawbacks, of course. Compared with regular authentication systems, such as passwords or tokens, which are precise, biometric authentication systems have probabilistic behavior. It turns out that there is no perfect match in biometrics; the authentication systems have to deal with error rates. These errors rates can vary by a number of factors. As an example, our voice vary drastically when we get sick or when we are under stress and this impacts a speaker authentication system. Aging, illumination, pose and face expressions are classical problems in face authentication systems, and these factors impacts the error rates of a face authentication systems.

The aforementioned problems and other issues are widely studied by the research community (Flynn, Jain & Ross 2008). To use a biometric trait in a biometric system, the candidate must satisfy the following requirements.

- Universality (every person must have it);
- Uniqueness (must distinguish people);
- Stability (must be stable along the time);
- Collectability (must be measure);
- Performance (must be relatively precise);

- Acceptance (the user must accept);
- Circumvention (low risk of frauds).

Table 2.1 shows a comparative between the most used biometric traits (Maltoni, Maio, Jain & Prabhakar 2009). It can be observed that none of the presented biometric traits fulfill all the listed requirements and the selection of a trait depends of some factors such as, the security requirements and the application purpose (Jain, Bolle & Pankanti 1999).

Table 2.1: Comparison of the most used biometric traits (Maltoni et al. 2009)

Biometric trait	Universality	Uniqueness	Stability	Coletability	Performance	Acceptance	Circumvention
Face	High	Low	Medium	High	Low	High	Low
Fingerprint	Medium	High	High	Medium	High	Medium	Medium
Hand geometry	Medium	Medium	Medium	High	Medium	Medium	Medium
Palm vein	Medium	Medium	Medium	Medium	Medium	Medium	High
Iris	High	High	High	Medium	High	Low	High
Signature	Low	Low	Low	High	Low	High	Low
Voice	Medium	Low	Low	Medium	Low	High	Low

2.2 Attacks in Biometric Systems

A regular biometric authentication system can be represented with the simple flow chart in Figure 2.1.

Firstly the biometric trait is captured using some sensor. Secondly the captured biometric trait is processed in order to extract the biometric features. When it is in an enrollment procedure, these features will generate a biometric reference, and it will be stored in a database. In an authentication procedure, these features will be used in a comparison with the stored biometric reference. It is possible to observe, in the same Figure, that attacks can be done in any point of the architecture (Xiao 2005). The next subsections discusses about each one of the possible point of attacks and how to mitigate it.

2.2.1 Replay attack

The replay attack is performed by injecting a biometric data previously sent, of the target identity, in order to have a non authorized access. This data can be obtained sniffing the biometric authentication software. To mitigate this kind of attack, the biometric system should ensure that the provided data was not injected artificially (Xiao 2005). The most popular way

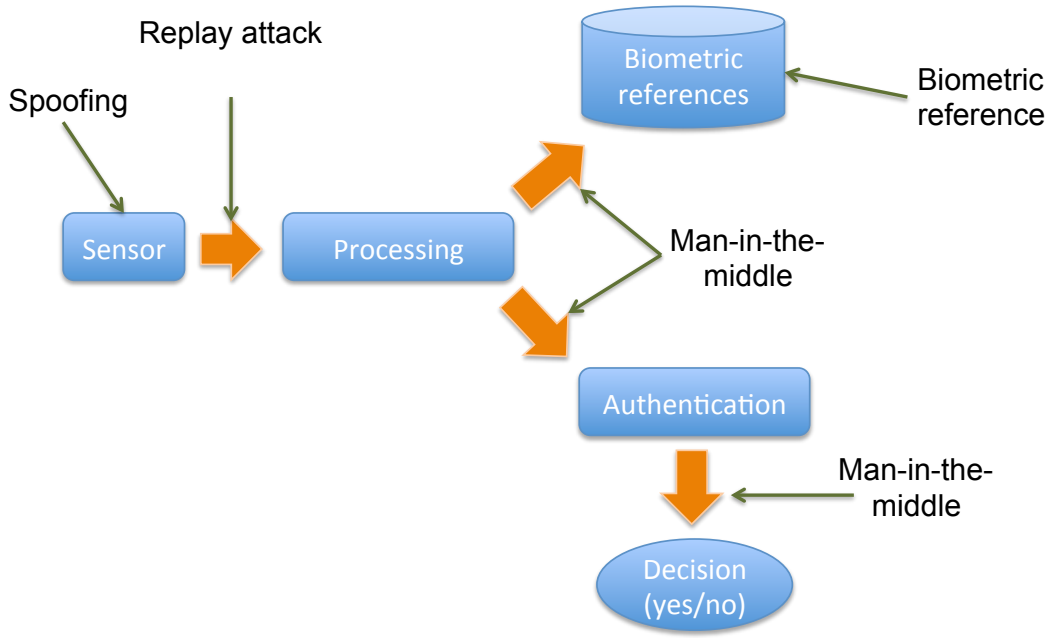


Figure 2.1: Simple architecture of a regular biometric authentication system (adapted from (Xiao 2005))

of protect this kind of attack is to associate a timestamp to the data. As it is improbable to have the exactly the same biometric data in different times, this method is quite effective.

2.2.2 Biometric reference attack

The attack in the biometric reference is performed where the biometrics are stored. This kind of attack include actions such as the inclusion, removing, modifying and steal biometric references. Among this actions, the possibility to steal a biometric reference is the most dangerous treat, since it is possible to work in a reverse engineering process to regenerate the biometric trait.

Using a hill climbing technique to optimize to the position and the orientation of the minutia (Martinez-Diaz, Fierrez-Aguilar, Alonso-Fernandez, Ortega-Garcia & Siguenza 2006) and (Hill 2001) shown that is possible to generate synthetic fingerprints compatible with fingerprints stored in a database. Fake fingers (with a real fingerprint) with gummy or silicon can be generated with this minutia. It is possible also to inject these minutia in the **Processing** module (Figure 2.1) in order to deceive the authentication system.

To mitigate the risk of this kind of attack best practices in security recommends to encrypt the biometric references and to increase the policy to access these biometric references.

2.2.3 Man-in-the-middle

In the man in the middle attack, the biometric data is intercepted in any point of the architecture in Figure 2.1. As shown in the Figure 2.1, the attacker can:

- Manipulate the matching score;
- Manipulate the biometric authentication response;
- Steal biometric data;
- Inject face biometric data (as shown in the Section 2.2.1).

The same security recommendations aforementioned to deal with this security breaks can be used here i.e. encrypt the data before transmission increase the security grants and so on.

2.2.4 Ataque de Spoofing

The spoofing attack in biometric system is a direct attack to the biometric sensor i.e. a forged biometric trait is presented to the biometric sensor. The goal is to pretend to be someone else in order to get some forbidden privileges. This type of attack is described with more details in Chapter 3.

Several technologies related to information security can be deployed in a biometric authentication system in order to mitigate the attacks aforementioned. We can highlight:

- Encrypt the biometric data;
- Traffic the biometric data using a secure channel;
- Deploy all modules of the architecture in a device that cannot be broken;
- Using more than one authentication factor.

However, in a spoofing attack, the target is the biometric sensor, and in the architecture presented in Figure 2.1, is not possible to apply any of the security tools to prevent this kind of attack, becoming the most fragile point. This kind of attack is the main point of this thesis.

2.3 Final Remarks

This chapter described the main concepts and the main threats that a biometric authentication system can suffer. As aforementioned, the biometric sensor is the most fragile point of threats in the architecture presented in the Figure 2.1. Countermeasures need to be studied in order to mitigate these threats. This masters thesis will deal with that topic.

Chapter 3

Spoofing Attacks

As aforementioned in the last chapter, spoofing attacks in biometrics are direct attacks to the biometric sensor. Spoofing techniques vary from different biometrics. This chapter discusses the spoofing attacks in different biometric traits focusing in face recognition. Section 3.1 presents the spoofing attacks in other biometric traits. Section 3.2 discusses spoofing in face biometrics. Section 3.3 presents the face antispoofing databases publicly available. Finally Section 3.4 presents the final remarks of the chapter.

3.1 Spoofing Attacks in Biometrics

Most of biometric systems can be spoofed. This section discusses the findings of spoofing attacks in different biometric systems.

3.1.1 Fingerprint

In fingerprints verification systems, the attacker can forge a fingerprint with different materials (gummy, silicone, etc). (Matsumoto, Matsumoto, Yamada & Hoshino 2002) and (Leyden 2002) discusses how to generate fake fingerprints using materials easily found in a supermarket. Figure 3.1 shows how easy is to create a mold from a live finger and to reproduce its fingerprint with gummy. This fake fingers can be used to spoof a fingerprint biometric systems.

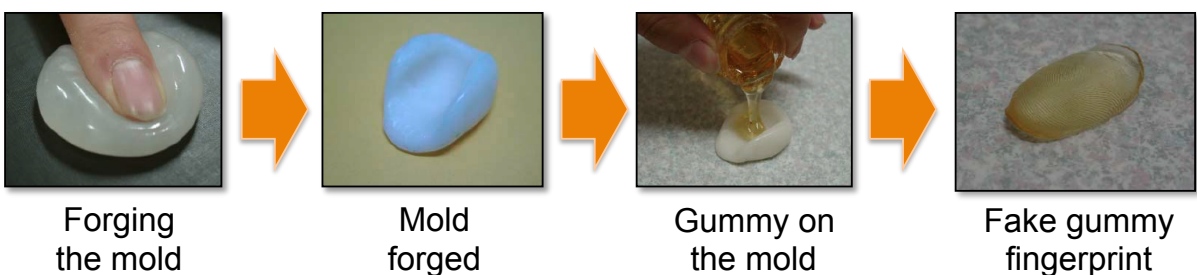


Figure 3.1: Creating a fake fingerprint (Adapted from (Matsumoto et al. 2002))

Recently in Brazil (2013), was reported that doctors in Sao Paulo were arrested after being caught in the act of using fake fingers made of silicone and imprinted with real fingerprints to defraud a hospital's biometric punch-in clock¹.

A more sophisticated attack were discussed in (Martinez-Diaz et al. 2006) and (Hill 2001). These papers use a hill climbing technique to optimize the position and the orientation of the minutia. With this optimization was possible to generate fingerprints compatible for match.

3.1.2 Speaker

For the speech biometrics the attacker can forge a human voice by mimicry or recording the voice of the target identity and replaying back to the microphone.

(Chetty & Wagner 2004) and (Eveno & Besacier 2005) address the problem using audio-visual features. The first one proposes a bi-modal authentication system using the face information in order to increase security. The second one correlates the lip movements with the content of the speech as a security barrier.

(Zhu, Chatlani & Soraghan 2012) analyses the speech signal itself applying the 1-dimensional *LBP* (Local Binary Pattern) followed by a SVM (Support Vector Machines) in order to detect spoofs.

3.1.3 Iris

Iris biometrics has been traditionally regarded as one of the most reliable and accurate biometric traits, but as the other biometric traits also can be spoofed. A simple way to spoof an iris recognition system is with a high quality printed image. More sophisticated attacks using contact lenses can also be carried out.

Countermeasures to deal with this kind of attacks can be deployed in the hardware level (with a specific equipment) or in the software level (Galbally, Ortiz-Lopez, Fierrez & Ortega-Garcia 2012). Specially in the software level, (Galbally et al. 2012) addresses the problem using a bunch of features, including a set of high pass filters, motion features and occlusion filters in the iris images followed by a binary classifier as countermeasure.

An approach based on textures was carried out by (Wei, Qiu, Sun & Tan 2008). This countermeasure uses the co-occurrence matrix descriptor followed by a binary classifier.

3.2 Spoofing Attacks in Face Recognition

Because of its natural and non-intrusive interaction, identity verification and recognition using facial information are among the most active and challenging areas in computer vision research. Despite the significant progress of face recognition technology in the recent decades, wide range of viewpoints, ageing of subjects and complex outdoor lighting are still research challenges. Advances in the area were extensively reported in (Flynn et al. 2008) and (Li & Jain 2011).

¹<http://www.foxnews.com/us/2013/03/13/brazilian-doctors-use-fake-silicone-fingers-to-defraud-hospital-punch-in-clock/>

It was not until very recently that the problem of spoofing attacks against face biometric system gained attention of the research community. This can be attested by the gradually increasing number of publicly available databases (Pan, Sun, Wu & Lao 2007, Tan, Li, Liu & Jiang 2010, Zhang, Yan, Liu, Lei, Yi & Li 2012, Chingovska, Anjos & Marcel 2012) and contests addressing the problem.

Two contests were organized in the last two years. The first one was organized under IJCB 2011 (International Joint Conference on Biometrics) (Chakka, Anjos, Marcel & Tronci 2011) which was the first competition conducted for studying best practices for non-intrusive spoofing detection. More recently, was organized the second competition in this field under ICB 2013 (International Conference on Biometrics).

In authentication systems based on face biometrics, spoofing attacks are usually perpetrated using photographs, videos or forged masks. While one can also use make-up or plastic surgery as mean of spoofing, photographs and videos are probably the most common sources of spoofing attacks. Moreover, due to the increasing popularity of social network websites (facebook, flickr, youtube, instagram and others), a great deal of multimedia content - especially videos and photographs - is available on the web that can be used to spoof a face authentication system. Figure 3.2 (a) and (b) shows the biometric data flow in a real access and in a spoofing attack respectively. In order to mitigate this kind of vulnerability in face authentication systems, effective countermeasures against face spoofing have to be deployed.

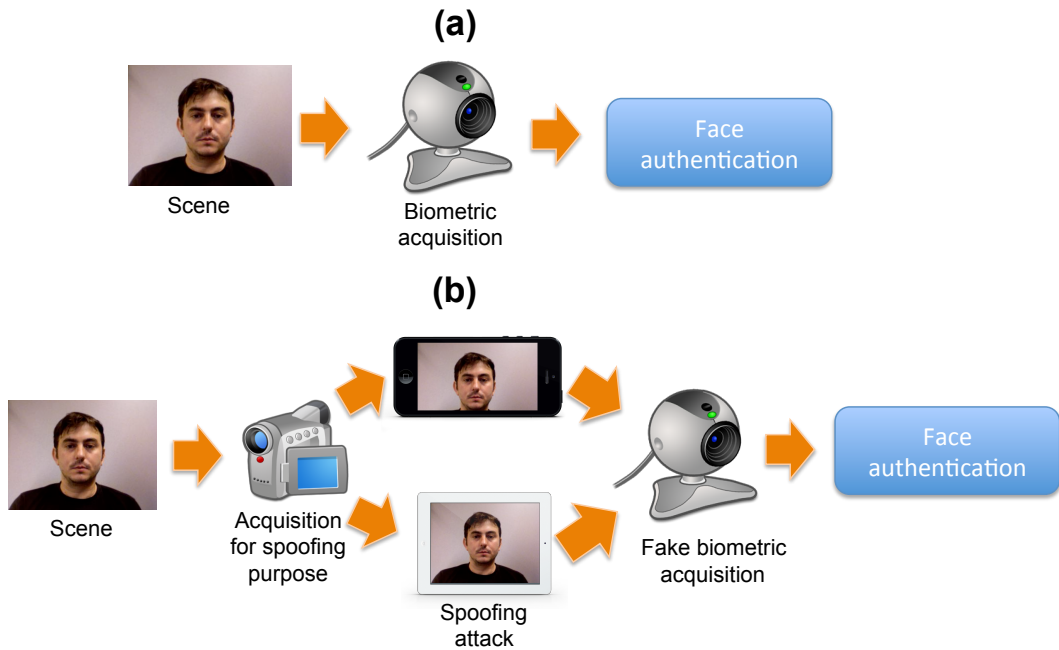


Figure 3.2: (a) Biometric data flow in a real access (b) Biometric data flow in a spoofing attack

Recently, the media has documented some situations of attacks in deployed face recognition systems. Using simple photographs, a research group from University of Hanoi showed how easy it is to spoof the face authentication systems deployed in Lenovo, Asus and Toshiba Laptops (Duc 2009). Since the release *Ice Cream Sandwich*, the Android OS come with a built-in

face authentication system to unlock the mobile phone. Since then, it has been extensively demonstrated around the web how easy it is to spoof this face recognition system². As a consequence, an eye blinking detection has been introduced in the most recent version of the Android OS.

The countermeasures against spoofing attempts in face recognition can be macro classified between the countermeasures that depends of user collaboration and the countermeasures that do not depends of user collaboration. The countermeasure that depends of user collaboration, the user is challenged to interact to the face authentication system. For example, researchers from google are studying a way to unlock the android phones based on facial expressions³. As can be observed in Figure 3.3, this strategy can be fun in the beginning but in some situations this can be embarrassing. On the other hand, the countermeasures that do not depend of user collaboration, try to solve this issue analysing the signal itself, without any awareness of the user. This type of countermeasures can be classified by the following cues:

- Presence of vitality (liveness detection);
- Scene characteristics;
- Differences in image quality assessment.



Figure 3.3: New google face unlock screen

3.2.1 Presence of vitality (liveness detection)

Presence of vitality or liveness detection, consists of search for features that only live faces can possess. The eye blinking is an activity that humans do constantly. A regular human blinks once every 2 or 4 seconds in order to maintain the eyes clean and wet. This frequency can vary in stress conditions and/or in a high concentration task. In that situations the interval can extend to ~ 20 seconds. However, doesn't matter in what condition the person is, in some point the eye blink will occur. Following that fact, (Pan et al. 2007) propose a countermeasure

²<http://www.itproportal.com/2011/11/14/ice-cream-sandwich-facial-recognition-cracked/>

³<http://www.bbc.co.uk/news/technology-22790221>

measuring the eye blinking using Hidden Markov Models (HMM) mapping the state of eyes open and closed. Experiments carried out using a database created by the authors and freely available for download⁴, shown an accuracy of 95.7% .

Supported by the hypothesis that live faces present uncorrelated motion patterns in some parts of the face compared to the attacks, (Kollreider, Fronthaler & Bigun 2009) developed a countermeasure based on optical flow field to explore such cue. As a reference to the algorithm, were selected the center of the face and the region of the ears, as can be observed in Figure 3.4.

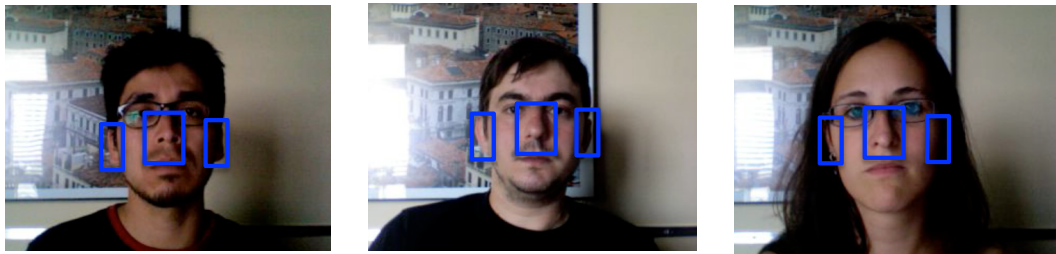


Figure 3.4: Selection of face regions of the algorithm (Kollreider et al. 2009)

The strategy of the countermeasure can be summarized as follows:

1. Detect the face region;
2. Delimitate the region of the face center and the ears (Figure 3.4);
3. Determine if the face region is moving more horizontally or more vertically analysing the optical flow velocities;
4. Compute the ratio between the velocities of the delimited areas of the face center and the ears;
5. The spoof is detected if the aforementioned ratio was bigger than a threshold α .

The performance was evaluated using an adaptation of the XM2VTS database. The real accesses were videos from XM2VTS database⁵ and the attacks were generated with printed photographs from the same database. With this database, which was not made public, an $EER = 0.5\%$ (Equal Error Rate) was achieved.

3.2.2 Scene

Countermeasures that search scene features analyse the relationship of the face in the scene.

The countermeasure proposed in (Anjos & Marcel 2011)⁶ measures the relative motion difference between the face and the background. The authors focused on simple differences of intensities in successive frames. The motion accumulated between this difference (M_D), for a

⁴http://www.cs.zju.edu.cn/gpan/database/db_blink.html

⁵<http://www.ee.surrey.ac.uk/CVSSP/xm2vtsdb/>

⁶<http://pypi.python.org/pypi/antispoofing.motion/>

given a Region-of-Interest (RoI) and its respective background, is computed using the following equation:

$$M_D = \frac{1}{S_D} \sum_{(x,y) \in D} |I_t(D) - I_{t-1}(D)|, \quad (3.1)$$

where D is the RoI, S_D is the area of the RoI and I_t is the intensity of a pixel.

To input the motion coefficient into a classifier, 5 quantities are extracted for every window of 20 frames. The quantities are: the minimum of M_D in that time window, the maximum, the average, the standard deviation and the ratio R between the spectral sum for all non-DC components and DC component itself taken as base the N -point Fourier transform of the signal (see Equation 3.2). These 5 quantities are fed into a Multi-layer Perceptron (MLP) classifier with 5 neurons in the hidden layer which is trained to detect spoofing attacks. This countermeasure was evaluated using the photograph attacks subset of the Replay Attack Database (Chingovska et al. 2012) and achieved an $HTER = 9\%$ (Half Total Error Rate).

$$R = \frac{\sum_{i=1}^N |FFT_i|}{|FFT_0|} \quad (3.2)$$

3.2.3 Differences in image quality assessment

Countermeasures based on differences in image quality assessment rely on the presence of artifacts intrinsically present at the attack media. Such remarkable properties can be originated from media quality issues or differences in reflectance properties of the object exposed to the camera.

Compared to real faces, attack medias have different reflexive patterns. Supported by that assumption, (Chingovska et al. 2012) and (Maatta and, Hadid & Pietikaandinen 2012), explored the *LBP* (Local Binary Patterns) texture descriptor analysing single frames. In this countermeasure the detected faces (see Figure 3.5) are geometric normalized to 64×64 pixels. The *LBP* features are extracted from the whole face region and histogrammed. The histograms for each frame are fed into a binary classifier which can be trained to detect spoofing attacks.

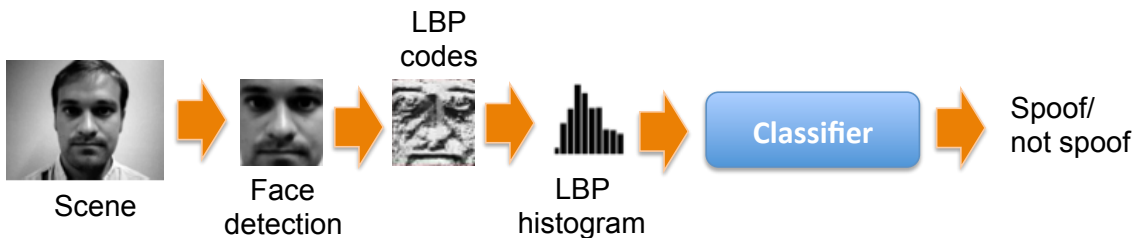


Figure 3.5: Block diagram of the countermeasure based on LBP

The Table 3.1 shows the reported performance, in $HTER$ terms, in the three databases; the Replay Attack Database, the CASIA FASD and the NUAA Database using the *SVM* (Support Vector Machines) and *LDA* (Linear Discriminant Analysis) as binary classifiers. It

can be observed a satisfactory performance in the three databases (between $\sim 15\%$ and $\sim 20\%$). However, comparing the performance in the development set (used to tune the hyperparameters) and in the test set of the NUAA database suggest a low generalisation capability.

Table 3.1: Performance in $HTER(\%)$ terms of the LBP countermeasure in three face spoofing databases.

	Replay Attack		NUAA		CASIA-FASD	
	dev set	test set	dev set	test set	dev set	test set
$LBP_{8,1}^{u2} + LDA$	19,60	17,17	0,06	18,32	17,08	21,01
$LBP_{8,1}^{u2} + SVM$	14,84	15,16	0,11	19,03	16,00	18,17

Supported by the assumption that images/videos used in attacks concentrates information in some specifics frequency bands, (Zhang et al. 2012) propose a countermeasure based on Difference of Gaussians filters (DoG).

As can be observed in the block diagram in Figure 3.6, four sequences of DoG filters are applied in the image. Each the gaussian kernel has the size 3×3 an it parameters are:

- $\sigma_1 = 0,5$ e $\sigma_2 = 1$;
- $\sigma_1 = 1$ e $\sigma_2 = 1,5$;
- $\sigma_1 = 1,5$ e $\sigma_2 = 2$;
- $\sigma_1 = 1$ e $\sigma_2 = 2$.

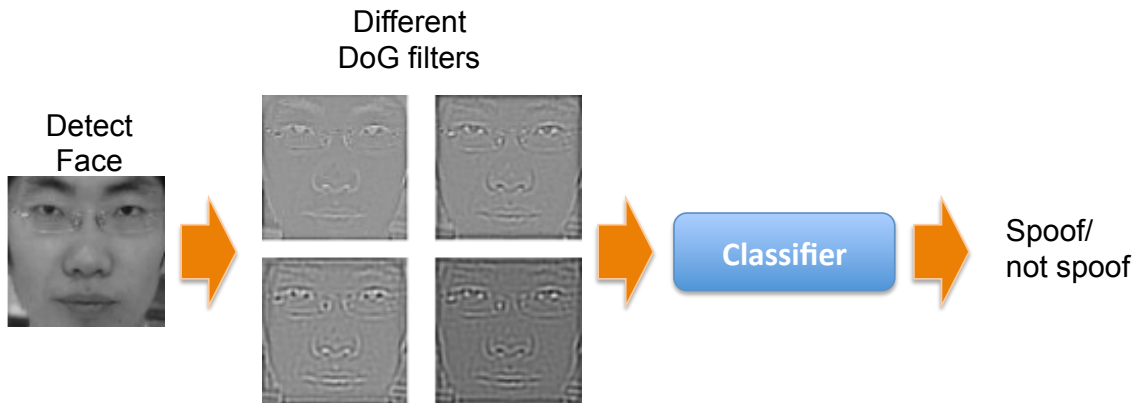


Figure 3.6: Block diagram of the DoG countermeasure

After of the sequence of filters, the images are geometric normalized to 128×128 pixels and these data fed into a SVM classifier. Evaluated using a the CASIA FASD, the countermeasure achieved an EER of 17%.

Li et al. (Li, Wang, Tan & Jain 2004) hypothesize that fraudulent photographs have less high frequency components than real ones. To test the hypothesis a small database was built with

4 identities containing both real access and printed photo attacks. With this private database, an accuracy of 100% was achieved.

In order to detect noise patterns in spoofing attacks, (da Silva Pinto, Pedrini, Schwartz & Rocha n.d.) developed a countermeasure analysing videos combining several elements. First, each frame in a frame sequence is filtered using a gaussian filter followed by a median filter. These filtered images are subtracted by the original ones. The result of this subtraction is so called "residual image". This residual image is analysed in the frequency domain using a 2D Fourier transform. All processed frames in the videos are combined using the Visual Rhythm technique(Zhang, Low, Smoliar & Wu 1995). This technique, generates one image with a combination of all frames ending the preprocessing steps.

A texture description using Gray Level Co-occurrence matrix (GLMC) was applied in the Visual Rhythm image. With the co-occurrence matrix, 12 measures are extracted to feed into a binary classifier that will detect attacks. The classifiers evaluated was the *PLS* (Partial Least Squares) and the *SVM*. With a database combining the photograph subset of the Replay Attack Database and a database created by the author (which was not made public), an AUC (Area Under the Curve) of $\sim 100\%$ was achieved.

3.3 Face Spoofing Databases

In this section, we give an overview of the only three face spoofing databases, the NUAA face antispoofing database, the Replay-Attack Database and the CASIA Face Anti-Spoofing Database (Zhang et al. 2012), consisting of real access attempts and several fake face attacks of different natures under varying conditions.

3.3.1 NUAA

The NUAA face spoofing database⁷ ?? consists of images of real accesses and attacks made with printed photographs. Emulating a scenario of access in a regular notebook, this database has images of 15 users split into 3 sections spaced over two weeks. Each section has 4 screenshots per user in different illumination conditions. Figure 3.7 has some examples of this database.



Figure 3.7: Printed photo attacks of the NUAA database

⁷<http://parnec.nuua.edu.cn/xtan/data/NuuaImposterdb.html>

3.3.2 Replay-Attack Database

The Replay-Attack Database⁴ (Chingovska et al. 2012) consists of short video ($\sim 10\text{s}$) recordings of both real-access and attack attempts to 50 different identities using a laptop. It contains 1200 videos (200 real-access and 1000 attacks) and the attacks were taken in three different scenarios with two different illumination and support conditions. The scenarios of attack include:

1. **print**: the attacker displays hard copies of high resolution photographs printed on A4 paper;
2. **mobile**: the attacker displays photos and videos taken with an iPhone 3GS using the phone screen;
3. **highdef**: The attacker displays high resolution photos and videos using an iPad screen with resolution 1024×768 .

The illumination conditions include:

1. **controlled**: the background of the scene is uniform and the light of a fluorescent lamp illuminates the scene;
2. **adverse**: the background of the scene is non uniform and the day-light illuminates the scene.

The support conditions include:

1. **hand-based**: the attacker holds the attack media using his own hands;
2. **fixed**: the attacker sets the attack device in a fixed support so it does not move during the spoofing attempt.

Figure. 3.8 show some examples of real accesses and attacks in different scenarios. In the top row, samples from controlled scenario. In the bottom row, samples from adverse scenario. Columns from left to right show examples of real access, printed photograph, mobile phone and tablet attacks.



Figure 3.8: Some frames of real access and spoofing attempts (courtesy of (Chingovska et al. 2012)).

Table 3.2: Number of videos in each subset. Numbers displayed as sums indicate the amount of hand-based and fixed support attack available in each subset.

Type	Train	Devel.	Test	Total
Real-access	60	60	80	200
Print-attack	30+30	30+30	40+40	100+100
Mobile-attack	60+60	60+60	80+80	200+200
Highdef-attack	60+60	60+60	80+80	200+200
Total	360	360	480	1200

The Replay-Attack database provides a protocol for objectively evaluate a given countermeasure. Such protocol defines three non-overlapping partitions for training, development (tuning) and testing countermeasures. The training set should be used to train the countermeasure, the development set is used to tune the countermeasure and to estimate a threshold value to be used in the test set. The test set must be used only to report results. As performance measurement, the protocol advises the use of Half Total Error Rate (HTER)(Equation 5.1).

$$HTER = \frac{FAR(\tau, D) + FRR(\tau, D)}{2}, \quad (3.3)$$

where τ is the decision threshold, D is the dataset, FAR is the False Acceptance Rate and FRR is the False Rejection Rate. In this protocol, the value of τ is estimated on the Equal Error Rate (EER) using the development set.

3.3.3 CASIA Face Anti-Spoofing Database

The CASIA Face Anti-Spoofing Database⁵ (Zhang et al. 2012) contains short videos of 50 real clients and the corresponding fake faces were captured with high quality from the original ones. The database has a variety kind of attack. This variety is achieved by introducing three imaging qualities (low, normal and high) and three fake face attacks which include warped photo, cut photo (eyeblink) and video attacks. Examples from the database can be seen in Figure 3.9. Altogether the database consists of 600 video clips and the subjects are divided into subsets for training and testing (240 and 360, respectively). Results of a baseline system are also provided along the database for fair comparison. The baseline system considers the high frequency information in the facial region using multiple DoG features and SVM classifier and is inspired by the work of Tan *et al.* (Tan et al. 2010).

Since the main purpose of the database is to investigate the possible effects of different fake face types and imaging qualities, the test protocol consists of seven scenarios in which particular train and test samples are to be used. The quality test considers the three imaging qualities separately, low (1), normal (2) and high quality (3), and evaluates the overall spoofing detection performance under variety of attacks at the given imaging quality. Similarly, the fake face test assesses how robust the anti-spoofing measure is to specific fake face attacks, warped photo (4), cut photo (5) and video attacks (6), regardless of the imaging quality. In the overall test (7),

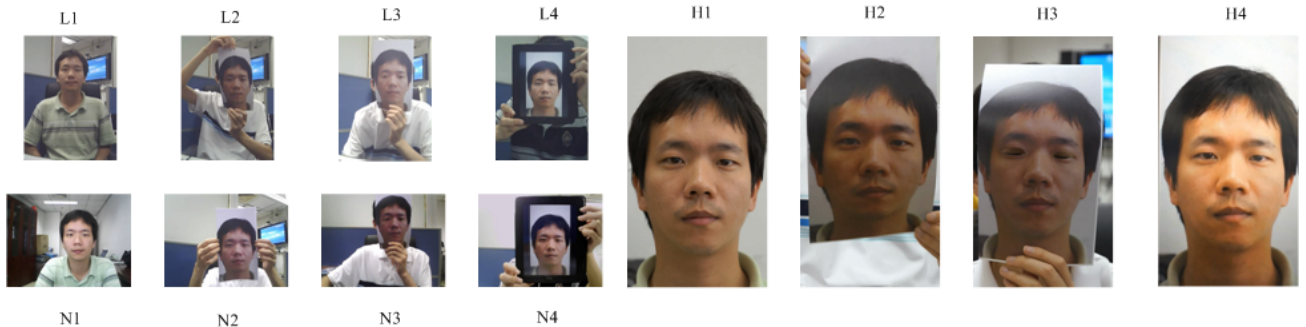


Figure 3.9: Example images of real accesses and the corresponding spoofing attempts (courtesy of (Zhang et al. 2012))

all data is used to give a more general evaluation. The results of each scenario are reported as Detection-Error Trade-off (DET) curves and equal error rates (EER), which is the point where false acceptance rate (FAR) equals false rejection rate (FRR) on the DET curve.

3.4 Final Remarks

In this chapter were exposed how it is possible to spoof biometric systems focusing in the face biometrics, the main issue of this masters project. The research community gave more attention in this kind of research mainly in the last three years. We can quote two evidences of this. The first one, two contest were organized in the last two years calling researchers to develop countermeasures. The second one; three databases were freely released in the last three years. The Section ?? shown that the most of the countermeasures presented in the literature were evaluated using different metrics and in some cases in private databases, make the work of comparison a hard task.

Chapter 4

Developed Countermeasures

TEXTO MOTIVANDO A CRIACAO DA CONTRAMEDIDA

4.1 LBP based dynamic texture description

Määttä et al. (Maatta and et al. 2012) and Chingovska et al. (Chingovska et al. 2012) propose a *LBP* based countermeasures to spoofing attacks based on the hypothesis that real faces present different texture patterns in comparison with fake ones. However, the proposed techniques analyse each frame in isolation, not considering the behaviour over time. As aforementioned, in the last chapter, motion is a cue explored in some works and in combination with texture can generate a powerful countermeasure. For describing the face liveness for spoofing detection, we considered a spatiotemporal representation which combines facial appearance and dynamics. We adopted the *LBP* based spatiotemporal representation because of its recent convincing performance in modelling moving faces and facial expression recognition and also for dynamic texture recognition (?).

The *LBP* texture analysis operator, introduced by Ojala et al. (?), is defined as a gray-scale invariant texture measure, derived from a general definition of texture in a local neighbourhood. It is a powerful texture descriptor and among its properties in real-world applications are its discriminative power, computational simplicity and tolerance against monotonic gray-scale changes. The original *LBP* operator forms labels for the image pixels by thresholding the 3×3 neighbourhood with the center value and considering the result as a binary number. The histogram of these $2^8 = 256$ different labels is then used as an image descriptor.

The original *LBP* operator was defined to only deal with the spatial information. However, more recently it has been extended to a spatiotemporal representation for dynamic texture analysis (DT). This has yielded to the so called Volume Local Binary Pattern operator (*VLBP*) (Zhao & Pietikainen 2007). The idea behind *VLBP* consists of looking at dynamic texture (video sequence) as a set of volumes in the (X, Y, T) space where X and Y denote the spatial coordinates and T denotes the frame index (time). The neighborhood of each pixel is thus defined in a three dimensional space. Then, similarly to basic *LBP* in spatial domain, volume textons can be defined and extracted into histograms. Therefore, *VLBP* combines motion and appearance into a dynamic texture description.

To make *VLBP* computationally treatable and easy to extend, the co-occurrences of the *LBP* on the three orthogonal planes (*LBP – TOP*) was also introduced (Zhao & Pietikainen 2007). *LBP – TOP* consists of the three orthogonal planes: *XY*, *XT* and *YT*, and the concatenation of local binary pattern co-occurrence statistics in these three directions. The circular neighbourhoods are generalized to elliptical sampling to fit to the space-time statistics. The *LBP* codes are extracted from the *XY*, *XT* and *YT* planes, which are denoted as *XY – LBP*, *XT – LBP* and *YT – LBP*, for all pixels, and statistics of the three different planes are obtained, and concatenated into a single histogram. The procedure is shown in Figure 4.1. In this representation, dynamic texture (DT) is encoded by the *XY – LBP*, *XT – LBP* and *YT – LBP*.

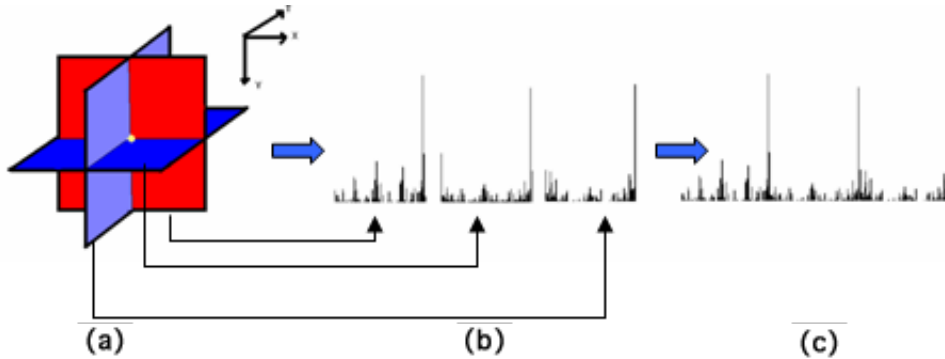


Figure 4.1: (a) Three planes intersecting one pixel (b) LBP histogram of each plane (c) Concatenating the histograms).

Using equal radii for the time and spatial axes is not a good choice for dynamic textures (Zhao & Pietikainen 2007) and therefore, in the *XT* and *YT* planes, different radii can be assigned to sample neighbouring points in space and time. More generally, the radii R_x , R_y and R_t respectively in axes X, Y and T, and the number of neighbouring points P_{XY} , P_{XT} and P_{YT} respectively in the *XY*, *XT* and *YT* planes can also be different. Furthermore, the type of *LBP* operator on each plane can vary, for example the uniform pattern (*u2*) or rotation invariant uniform pattern (*riu2*) variants (?) can be deployed. The corresponding feature is denoted as $LBP - TOP_{P_{XY}, P_{XT}, P_{YT}, R_x, R_y, R_t}^{operator}$.

Assuming we are given a $X \times Y \times T$ dynamic texture ($x_c \in \{0, \dots, X-1\}$, $y_c \in \{0, \dots, Y-1\}$, $t_c \in \{0, \dots, T-1\}$), i.e. a video sequence. An histogram of the DT can be defined as:

$$H_{i,j} = \sum_{x,y,t} I\{f_j(x,y,t) = i\}, \quad i = 0, \dots, n_j - 1; j = 0, 1, 2. \quad (4.1)$$

where n_j is the number of different labels produced by the *LBP* operator in the j_{th} plane ($j = 0 : XY$, $1 : XT$ and $2 : YT$), $f_i(x,y,t)$ expresses the *LBP* code of central pixel (x,y,t) in the j_{th} plane and I is defined as follows:

$$I(A) = \begin{cases} 1 & \text{if } A \text{ is true} \\ 0 & \text{if } A \text{ is false.} \end{cases} \quad (4.2)$$

Similarly to the original LBP, the histograms must be normalized to get a coherent description for comparing the DTs:

$$N_{i,j} = \frac{H_{i,j}}{\sum_{k=0}^{n_j-1} H_{k,j}} . \quad (4.3)$$

In addition to the computational simplification, compared with *VLBP*, *LBP-TOP* has the advantage to generate independent histograms for each of intersecting planes, in space and time, which can be treated in combination or individually. Because of the aforementioned complexity issues on the implementation of a *VLBP* based processor, the developed spatiotemporal face liveness description uses *LBP-TOP* to encode both facial appearance and dynamics.

Our key idea is to learn and detect the structure and the dynamics of the facial micro-textures that characterise real faces but not fake ones. Due to its tolerance against monotonic gray-scale changes, *LBP* based representation is adequate for measuring the facial texture quality and determining whether degradations due to recapturing process, e.g. the used spoofing medium, are observed. Instead of just applying static texture analysis, we exploit also several dynamic visual cues that are based on either the motion patterns of a genuine human face or the used display medium.



Figure 4.2: Example sequence of a warped photo attack from the CASIA Face Anti-Spoofing Database ZHANG describing the characteristic reflections (flickering) of planar spoofing medium and the distorted motion patterns.

Unlike photographs and display devices, real faces are indeed non-rigid objects with contractions of facial muscles which result in temporally deformed facial features such as eye lids and lips. Therefore, it can be assumed that the specific facial motion patterns (including eye blinking, mouth movements and facial expression changes) should be detected when a live human being is observed in front of the camera. The movement of the display medium may cause several distinctive motion patterns that do not describe genuine faces. As shown in Figure 4.2, the use of (planar) spoofing medium might cause sudden characteristic reflections when a photograph is warped or because of a glossy surface of the display medium. As it can be seen, warped photo attacks may cause also distorted facial motion patterns. It is likely that hand-held attacks introduce synchronized shaking of the face and spoofing medium which can be observed as excessive relative motion in the view and facial region if the distance between the display medium and the camera is relatively short. This countermeasure try to exploit the aforementioned visual cues for face spoofing detection by exploring the dynamic texture content

of the facial region. We adopted the *LBP* based spoofing detection in spatiotemporal domain because *LBP – TOP* features have been successfully applied in describing dynamic events, e.g. facial expressions (Zhao & Pietikainen 2007).

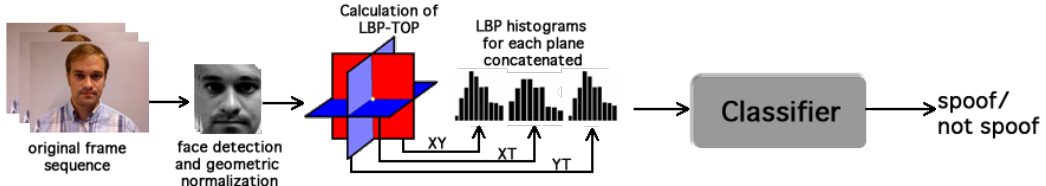


Figure 4.3: Block diagram of the proposed countermeasure.

4.2 Architecture of the countermeasure

Figure 4.3 shows a block diagram of the proposed countermeasure. First, each frame of the original frame sequence was gray-scaled and passed through a face detector using Modified Census Transform (*MCT*) features (Froba & Ernst 2004). Only detected faces with more than 50 pixels of width and height were considered. The detected faces were geometric normalized to 64×64 pixels. In order to reduce the face detector noise, the same face bounding box was used for each set of frames used in the *LBP – TOP* calculation. As can be seen in the Figure 4.4, the middle frame was chosen. Unfortunately, the face detector is not error free and in case of error in the middle frame face detection, the nearest detection was chosen; otherwise the observation was discarded. After the face detection step, the *LBP* operators were applied for each plane (*XY*, *XT* and *YT*) and the histograms were computed and then concatenated. After the feature extraction step, binary classification can be used to discriminate spoofing attacks from real access attempts.

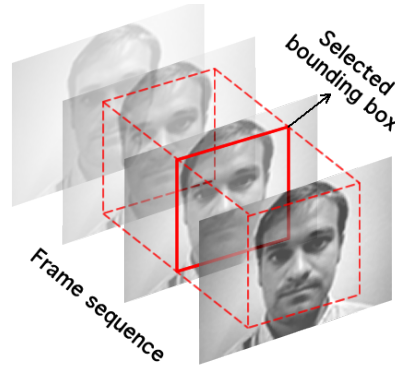


Figure 4.4: Face detection strategy for $R_t = 1$.

Face liveness is rather difficult to be determined based on the motion between couple of successive frames. The used volume can be expanded along the temporal dimension by increasing

R_t , as aforementioned in section 4.1. This way to deal with dynamic texture is called single resolution approach, since only one histogram per $LBP - TOP$ plane is accumulated. However, this leads to rather sparse sampling on the temporal planes XT and YT , thus we might loose valuable details. In order to explore the dynamic texture information more carefully, we proposed the multiresolution approach.

The multiresolution approach can be performed by concatenating the histograms in the time domain (XT and YT) for different values of R_t . The notation chosen to represent these settings is using brackets for the multiresolution data. For example, $R_t = [1 - 3]$ means that the $LBP - TOP$ operator will be calculated for $R_t = 1$, $R_t = 2$ and $R_t = 3$ and all resultant histograms will be concatenated. With the multiresolution approach, dense sampling on the temporal planes XT and YT is achieved.

4.3 Experiments

This section provides an in-depth analysis on the proposed $LBP - TOP$ based face liveness description using the Replay-Attack Database (Chingovska et al. 2012) and the CASIA Face Anti-Spoofing Database (Zhang et al. 2012). First, we study the effect of different classifiers and $LBP - TOP$ parameters by following the evaluation method proposed in (?). The $LBP - TOP$ representation is computed over relatively short temporal windows and the results are reported using the overall classification accuracy for the individual volumes. Altogether four experiments were carried out evaluating the effectiveness of:

1. Each $LBP - TOP$ plane individually and in combination;
2. Different classifiers;
3. Different LBP operators;
4. The multiresolution approach.

In order to study the effect of the different variables, each parameter was tuned solely (fixing other elements) using the development set of each face spoofing database. It should be noted that unlike the Replay-Attack Database, the CASIA Face Anti-Spoofing Database is lacking a specific development set. Therefore, the first four experiments were performed in this database using cross-validation by randomly dividing the training data into five folds. Hence, the results presented for CASIA Face Anti-Spoofing Database are actually the average $HTER$ on the test set over five iterations of the algorithm with different folds playing the role of a development set.

Finally, we also studied the accumulation of facial appearance and dynamics information over longer time windows and perform an evaluation at system level. The access attempt based results presented in Section 4.3.5 were obtained using the official protocol of each database.

Inspired by (Chingovska et al. 2012), the $LBP - TOP$ operator chosen to start the evaluation was $LBP - TOP_{8,8,8,1,1,R_t}^{u2}$.

4.3.1 Effectiveness of each $LBP-TOP$ plane individually and in combination

In this experiment, we analysed the effectiveness of each individual plane and their combinations when the multiresolution area is increased. Figure 4.5 shows the $HTER$ evolution, on the test set, considering individual and combined histograms of $LBP-TOP$ planes for each database. We used, as binary classifier, a linear projection derived from Linear Discriminant Analysis LDA as in (Chingovska et al. 2012).

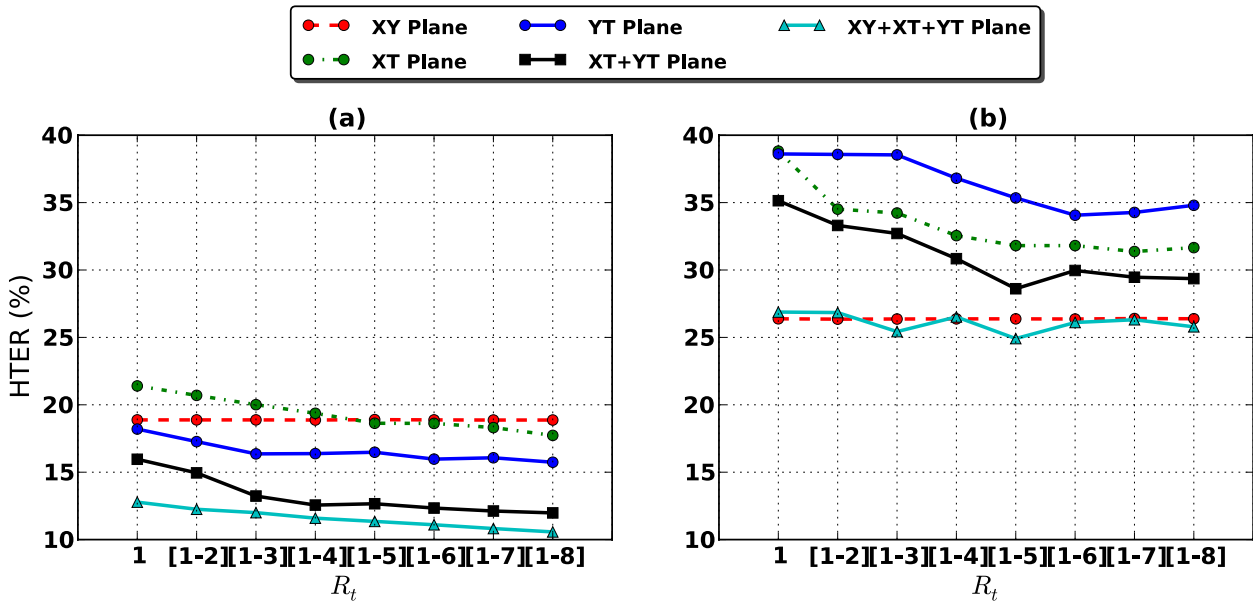


Figure 4.5: (Color online) Evaluation of $HTER(\%)$ in each plane when the multiresolution area (R_t) is increased with $LBP-TOP_{8,8,8,1,1,R_t}^{u^2}$ and LDA classifier - test-set **(a)** Replay-Attack Database **(b)** CASIA Face Anti-Spoofing Database.

The results indicate differences in the performance between the two databases. The temporal components (XT and YT) are a decisive cue for the Replay-Attack Database and the combination of all three planes (XY , XT and YT) gives the best performance. Conversely, for the CASIA Face Anti-Spoofing Database, the addition of temporal planes improves the performance only slightly compared to the spatial LBP representation (considering only the XY plane). These observations can be explained by taking a closer look at the differences in the databases and their spoofing attack scenarios. 2D fake face attacks can be categorized into two groups, close-up and scenic attacks, based on how the fake face is represented with the spoofing medium.

A close-up spoof describes only the facial area which is presented to the sensor. The main weakness with the tightly cropped fake faces is that the boundaries of the spoofing medium, e.g. a video screen frame, photograph edges, or the attacker's hands are usually visible during the attack, thus can be detected in the scene (Komulainen 2012). However, these visual cues can be hidden by incorporating background scene in the face spoof and placing the resulting scenic

fake face very near to the sensor as performed on the Replay-Attack Database. In such cases, the description of facial appearance leads to rather good performance because the proximity between the spoofing medium and the camera causes the recaptured face image to be out-of-focus also revealing other facial texture quality issues, like degradation due to the used spoofing medium. Furthermore, the attacks in Replay-Attack Database are performed using two types of support conditions, fixed and hand-held. Naturally, the $LBP - TOP$ based face representation can easily detect fixed photo and print attacks since there is no variation in the facial texture over time. On the other hand, the hand-held attacks introduce synchronized shaking of the face and spoofing medium. This can be observed as excessive relative motion in the view, again, due to the proximity between the display medium and the sensor. Since the distinctive global motion patterns are clearly visible also on the facial region, they can be captured even by computing the LBP-TOP description over relatively short temporal windows, i.e. low values of R_t .

In contrast, the CASIA Face Anti-Spoofing database consists of close-up face spoofs. The distance between the camera and the display medium is much farther compared to the attacks on Replay-Attack Database. The display medium does not usually move much in the attack scenarios. Therefore, the overall translational movement of a fake face is much closer to the motion of a genuine head. Due to the lack of distinctive shaking of the display medium, the CASIA Face Anti-Spoofing Database can be considered to be more challenging from the dynamic texture point of view. Because the motion cues are harder to explore in some attack scenarios using small values of R_t , we investigated in Section 4.3.5 whether the use of longer time windows helps to reveal the disparities between a genuine face and a fake one.

4.3.2 Effectiveness of different classifiers

In this experiment, we analysed the effectiveness of different classifiers when the multiresolution area is increased. Fig. 4.6 shows the HTER evolution, on the test set, under three different classifications schemes. The first one uses χ^2 distance, since the feature vectors are histograms. The same strategy reported in (Chingovska et al. 2012) was carried out. A reference histogram only with real accesses was created averaging the histograms in the training set. The last two selected classification schemes analysed were: Linear Discriminant Analysis (LDA) and Support Vector Machines (SVM) with a radial basis function kernel (RBF).

The SVM classifier with an RBF kernel provided the best performance on the Replay-Attack Database and the CASIA Face Anti-Spoofing Database (7.97% and 20.72% in terms of HTER, respectively). However, it is important to remark that the same LBP-TOP configuration with an LDA classifier resulted in comparable performance (11.35% and 24.91% in terms of HTER). This is not a huge gap and the classification scheme is far simpler. As similar findings have been reported (Chingovska et al. 2012, ?), the use of simple and computationally efficient classifiers should be indeed considered when constructing real-world anti-spoofing solutions.

4.3.3 Effectiveness of different LBP operators

The size of the histogram in a multiresolution analysis, in time domain, increases linearly with R_t . The choice of an appropriate LBP representation in the planes is an important issue since it

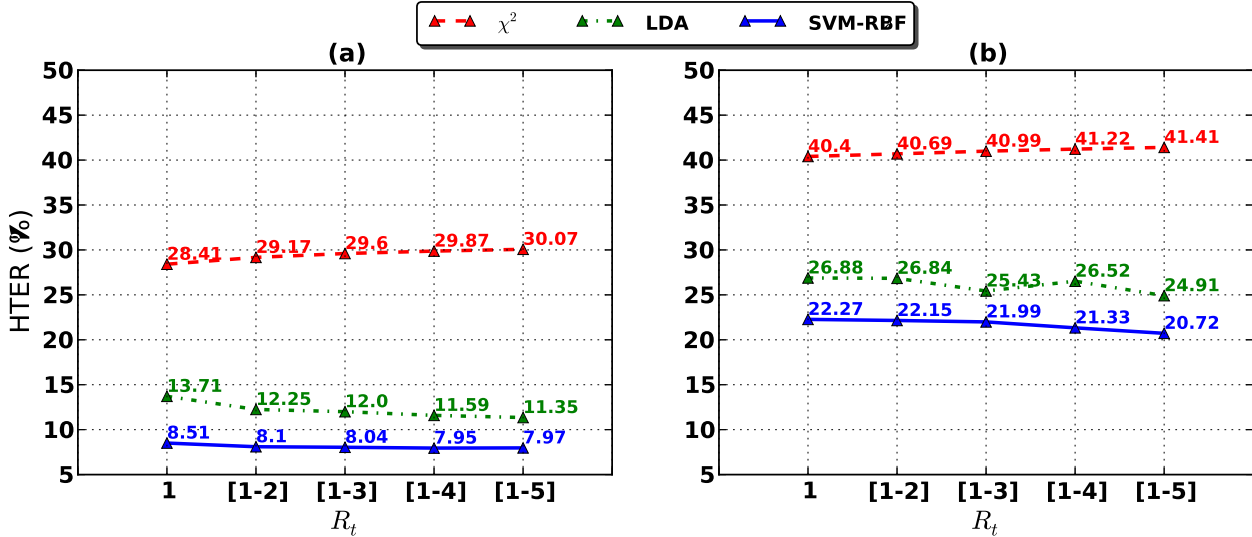


Figure 4.6: (Color online) Evaluation of HTER(%) with $\text{LBP-TOP}_{8,8,8,1,1,R_t}^{u2}$ using different classifiers (a) Replay-Attack Database (b) CASIA Face Anti-Spoofing Database.

impacts the size of the histograms. Using uniform patterns or rotation invariant extensions, in one or multiple planes, may bring a significant reduction in computational complexity. In this experiment, the effectiveness of different LBP operators in the three LBP-TOP planes (XY , XT and YT) was analysed. Fig. 4.7 shows the performance, in HTER terms, configuring each plane as basic LBP (with 256 bins for $P = 8$), LBP^{u2} (uniform patterns) and LBP^{riu2} (rotation invariant uniform patterns) when the multiresolution area (R_t) is increased in both databases. Results must be interpreted with the support of Fig. 4.8, which shows the number of bins on the histograms used for classifications in each configuration.

When the multiresolution area is increased, the HTER saturates for LBP^{riu2} and LBP^{u2} on both datasets. For the basic LBP operator a minimum can be observed in 7.60% and 20.71% on the Replay-Attack Database and CASIA Face Anti-Spoofing Database respectively. On both databases, basic LBP and LBP^{u2} presented similar performance. Even though the use of regular LBP leads to the best results, the LBP^{u2} operator seems to provide a reasonable trade-off between computational complexity (see Fig. 4.8) and performance. Hence, we will still proceed with LBP^{u2} .

4.3.4 Effectiveness of the multiresolution approach

In this experiment we analysed the effectiveness of the multiresolution approach in comparison with the single resolution approach. The single resolution approach consists of using only fixed values for R_t , without concatenating histograms for each R_t . With this approach the size of the histograms will be constant for different values of R_t , which decreases the computational complexity compared to the multiresolution approach. Fig. 4.9 shows the HTER evolution for different values of R_t in both databases comparing the both approaches.

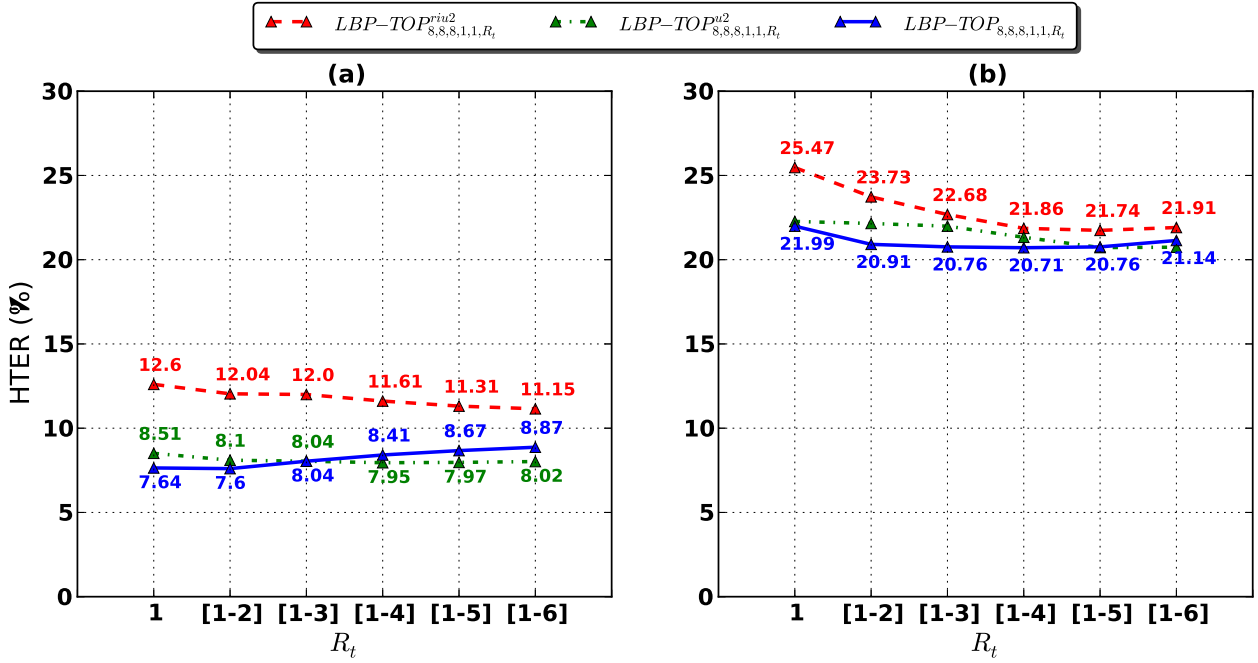


Figure 4.7: (Color online) Evaluation of HTER(%) with LBP-TOP_{8,8,8,1,1,R_t} using different LBP configurations in the planes with SVM classifier **(a)** Replay-Attack Database **(b)** CASIA Face Anti-Spoofing Database.

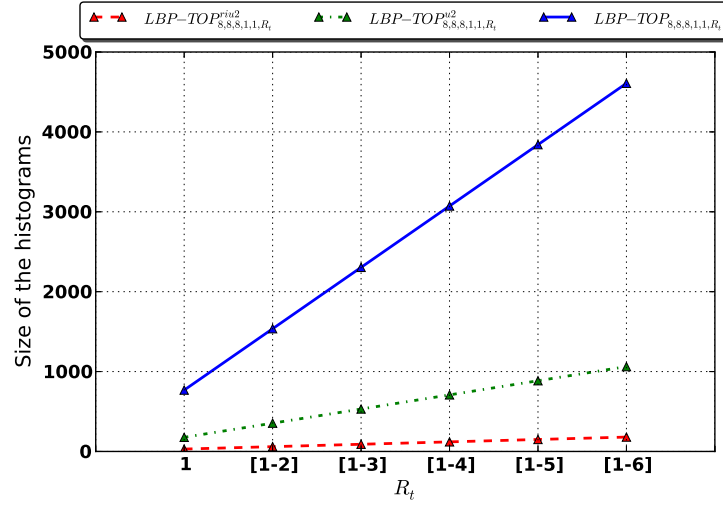


Figure 4.8: (Color online) Evaluation of the histogram size when (R_t) is increased.

On both datasets, the HTER of single resolution approach increases with R_t whereas the multiresolution approach helps to keep the HTER low when the multiresolution area is increased. This suggests that the increase of R_t causes more sparse sampling in the single resolution approach when valuable motion information is lost. In contrary, the more dense sampling of the

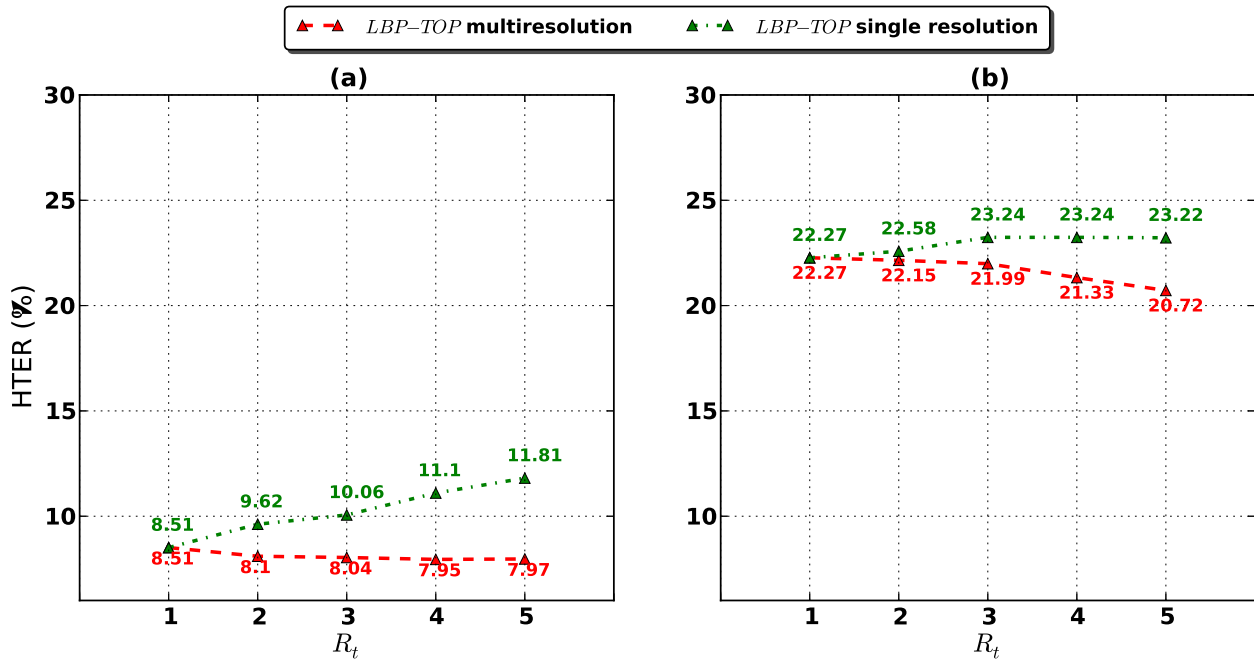


Figure 4.9: (Color online) Evaluation of HTER% using $\text{LBP-TOP}_{8,8,1,1,R_t}^{u2}$ with the single resolution and the multiresolution approach using SVM classifier (a) Replay-Attack Database (b) CASIA Face Anti-Spoofing Database.

multiresolution approach is able to provide a more detailed description of the motion patterns, thus improving the discriminative power.

4.3.5 Access attempt based analysis

In the previous experiments, the importance of the temporal dimension was studied using the single resolution and the multiresolution approaches. As seen in Section 4.3.1, the multiresolution approach is able to capture well the nature of fixed photo attacks and the excessive motion of display medium, especially on the Replay-Attack Database. However, in some attack scenarios, the motion patterns were harder to explore using small values of R_t . Therefore, we now study how the used temporal window size affects the performance when the facial appearance and dynamics information are accumulated over time. The face description of the single resolution and multiresolution methods can be accumulated over longer time periods either by averaging the features within a time window or by classifying each subvolume and then averaging the scores within the current window. In this manner, we are able to provide dense temporal sampling over longer temporal windows without excessively increasing the size of the feature histogram.

To follow the method used in previous experiments, we begin evaluating the two averaging strategies with the $\text{LBP-TOP}_{8,8,1,1,1}^{u2}$ operator and a SVM classifier with RBF kernel. In order to determine the video based system performance, we applied both average of features and scores on the first valid time window of N frames from the beginning of each video sequence. It

should be noted that the following access attempt based analysis is based on the official protocol of each database. Thus, the results on Replay-Attack Database are reported in terms of HTER whereas the performance on CASIA Face Anti-Spoofing Database is described using EER.

The access attempt based performance of both averaging strategies on the two databases is presented in Fig. 4.10. The results indicate that when the amount of temporal information increases, the better we are able to discriminate real faces from fake ones. This is the case especially on the CASIA Face Anti-Spoofing Database in which the distinctive motion clues, such as the excessive shaking of the display medium, cannot be exploited. However, when longer video sequences are explored, we are more likely to observe other specific dynamic events, such as different facial motion patterns (including eye blinking, lip movements and facial expression changes) or sudden characteristic reflections of planar spoofing media which can be used for differentiating real faces from fake ones. It is also interesting to notice that by averaging features, more stable and robust spoofing detection performance is achieved on both databases. The averaging scores of individual subvolumes seems to suffer from outliers, thus more sophisticated temporal processing of scores might lead to more stable behaviour.

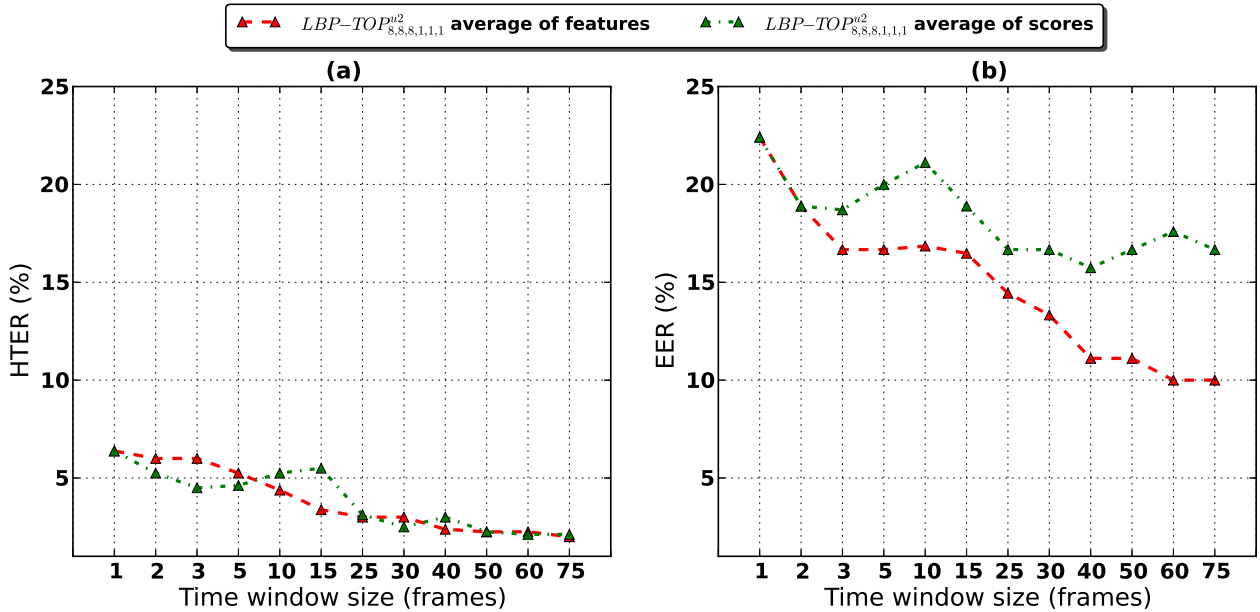


Figure 4.10: (Color online) Access attempt based evaluation of different time window sizes using mean of features and mean of scores with LBP-TOP_{8,8,8,1,1,1} (a) Replay-Attack Database (HTER %) (b) CASIA Face Anti-Spoofing Database (EER %).

According to the official test protocol of CASIA Face Anti-Spoofing, also the Detection-Error Trade-off (DET) curves and the EERs for the seven scenarios should be reported. Based on the previous analysis we chose to use the average of features within a time window of 75 frames which corresponds to three seconds of video time. As it can be seen in Fig 4.11 and Table 4.1, the use of only facial appearance (LBP) leads to better results compared to the baseline method (CASIA baseline). More importantly, when the temporal planes XT and YT

Table 4.1: EER (in %) comparison between the DoG baseline method, $LBP_{8,1}^{u2}$ and $LBP\text{-TOP}_{8,8,8,1,1,1}^{u2}$ using average of features on the CASIA Face Anti-Spoofing Database.

Scenario	Low	Normal	High	Warped	Cut	Video	Overall
DoG baseline (Zhang et al. 2012)	13	13	26	16	6	24	17
$LBP_{8,1}^{u2}$	11	17	13	13	16	16	16
$LBP\text{-TOP}_{8,8,8,1,1,1}^{u2}$	10	12	13	6	12	10	10

are also considered for spatiotemporal face description (LBP-TOP), a significant performance enhancement is obtained (from 16% to 10% in terms of EER), thus confirming the benefits of encoding and exploiting not only the facial appearance but also the facial dynamics information.

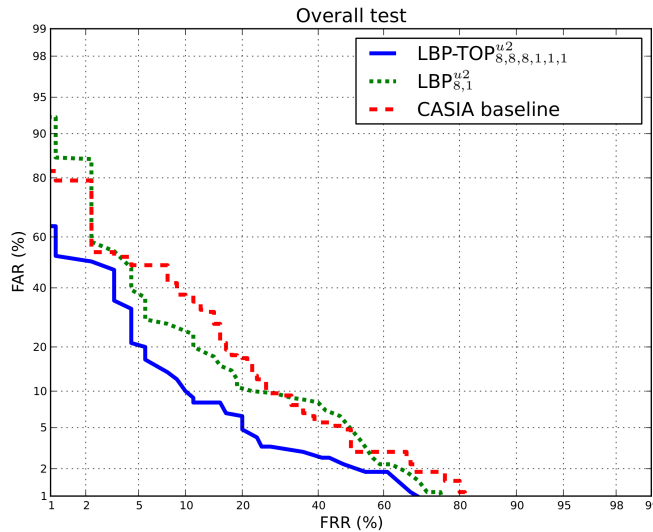


Figure 4.11: (Color online) Overall performance of $LBP\text{-TOP}_{8,8,8,1,1,1}^{u2}$ using average of features compared to the DoG baseline method and $LBP_{8,1}^{u2}$ on the CASIA Face Anti-Spoofing Database.

More detailed results for each scenario are presented in Fig. 4.12 and in Table 4.1. The results indicate that the proposed LBP-TOP based face description yields best results in all configurations except under cut-photo attacks. As described in (Zhang et al. 2012), the DoG filtering baseline method is able to capture the less variational nature of the cut eye regions well. However, the difference in the motion patterns seems to be too small for our LBP-TOP based approach as mainly eye blinking occurs during the cut-photo attacks and no other motion is present. The EER development presented in Table 4.2 supports this conclusion since the performance under cut-photo attacks does not improve that much if longer temporal window is applied compared to the other scenarios.

On the other hand, the spatiotemporal face description is able to improve the major drawbacks of DoG based countermeasure. Unlike the baseline method, our approach performs almost equally well at all three imaging qualities. Furthermore, the performance under warped photo

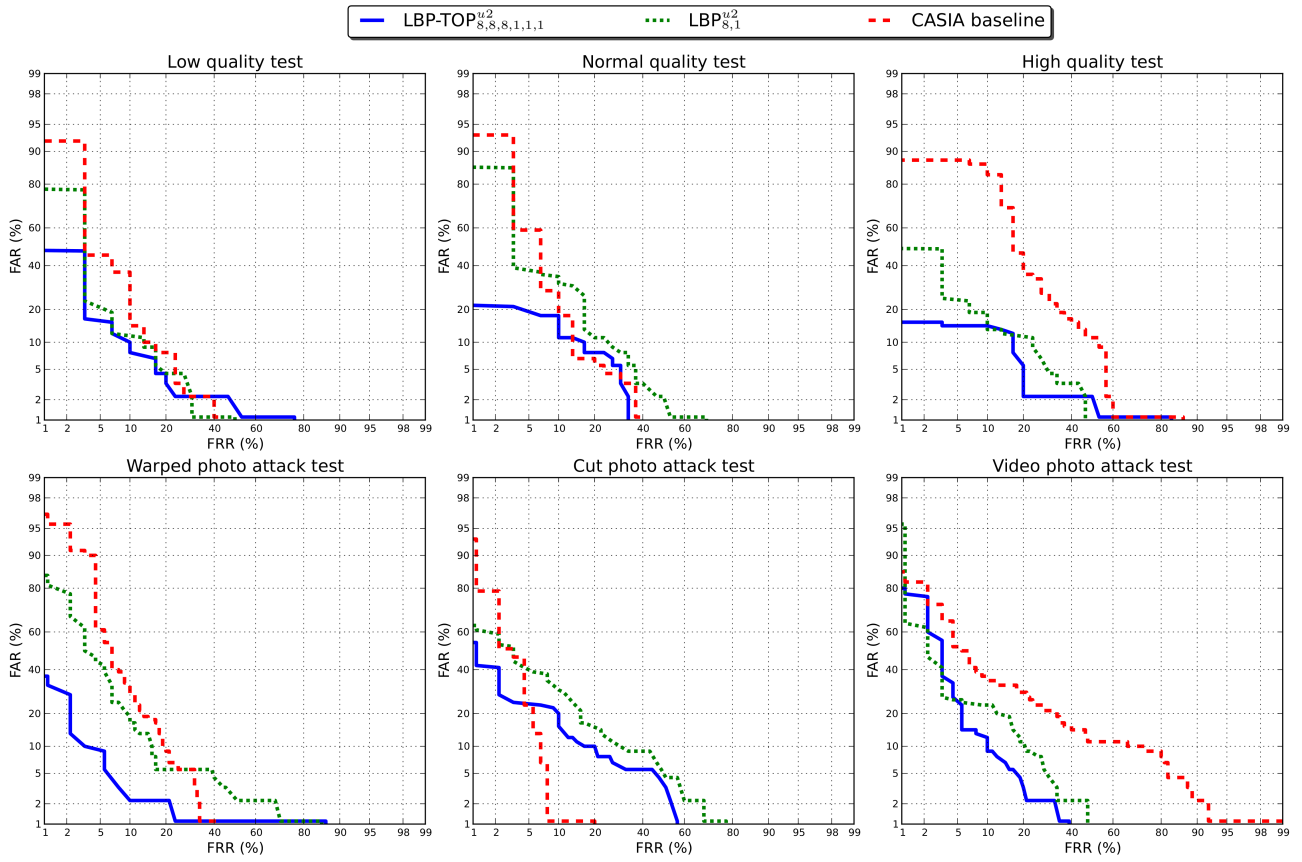


Figure 4.12: (Color online) Performance of LBP-TOP^{u2}_{8,8,8,1,1,1} using average of features compared to the DoG baseline method and LBP^{u2}_{8,1} under the different protocols of the CASIA Face Anti-Spoofing Database.

and video attacks is significantly better. Especially the characteristic specular reflections (flickering) and excessive and distorted motion of warped photo attacks can be described very well.

4.3.6 Summary

Table 4.3 and Table 4.4 summarize all the results obtained for each database following their provided protocols. In order to be comparable with still frame analysis presented for example in (Chingovska et al. 2012), the results for Replay-Attack Database represent the overall classification accuracy considering each frame individually. The access attempt based results are reported only for CASIA Face Anti-Spoofing Database as requested in its test protocol.

Table 4.3 shows also the results for the LBP⁶ (Chingovska et al. 2012) and the Motion Correlation⁷ (Anjos & Marcel 2011) based countermeasures whose source code is freely available. Table 4.4 contains the provided DoG based baseline and the holistic LBP based face description. It can be seen that the proposed countermeasure presented the best results overtaking the baseline results in both databases, thus confirming the benefits of encoding and exploiting not only the facial appearance but also the facial dynamics information. Unfortunately, our comparison is limited to these countermeasures due to the lack of publicly available

Table 4.2: EER (in %) development of LBP-TOP $^{u2}_{8,8,8,1,1,1}$ using average of features on the CASIA Face Anti-Spoofing Database.

Frames	Low	Normal	High	Warped	Cut	Video
1	17	27	23	29	16	20
5	13	20	20	19	14	14
10	14	20	19	18	16	14
25	13	13	10	10	14	12
50	13	11	10	7	13	10
75	10	12	13	6	12	10

Table 4.3: HTER(%) of the best results achieved on the Replay-Attack Database (following the database protocol) comparing with the provided baseline.

	dev	test
Motion Correlation (Anjos & Marcel 2011)	11.78	11.79
LBP $^{u2}_{8,1}$ + SVM	14.84	15.16
LBP $_{3\times 3}$ + SVM (Chingovska et al. 2012)	13.90	13.87
LBP-TOP $^{u2}_{8,8,8,1,1,1}$ + SVM	8.17	8.51
LBP-TOP $_{8,8,8,1,1,[1-2]}$ + SVM	7.88	7.60

implementations of other state-of-the-art techniques presented in literature.

During these experiments we observed that the general performance of the proposed countermeasure was consistently better on Replay-Attack Database compared to the CASIA Face Anti-Spoofing Database. As mentioned in Section 4.3.1, the nature of the attack scenarios is different between the two datasets. In the Replay-Attack Database, our LBP-TOP based face description was able to capture motion patterns of fixed photo attacks and scenic fake face attacks already when only relatively short time windows were explored. Performances below 10% (HTER) were achieved. On the other hand, the CASIA Face Anti-Spoofing Database turned out to be more challenging from the dynamic texture point of view. Due to the lack of motion, analysis of longer temporal windows was required in order to find out distinctive motion patterns between genuine faces and fake ones. As it can be seen in Table 4.4, by extending the micro-texture based spoofing detection into spatiotemporal domain, an improvement from 16% to 10% in terms of EER was obtained. The results also indicate that the proposed dynamic texture based face liveness description was able to improve the state of the art on both datasets.

4.4 Final Remarks

Inspired by the recent progress in dynamic texture, the problem of face spoofing detection was investigated in this chapter using spatiotemporal local binary patterns. The key idea of the proposed countermeasures consists of analysing the structure and the dynamics of the micro-

Table 4.4: $EER(\%)$ of the best results achieved on the CASIA Face Anti-Spoofing Database (following the database protocol) comparing with the provided baseline.

	test
DoG baseline (Zhang et al. 2012)	17
LBP $_{8,1}^{u2}$ + SVM	16
LBP-TOP $_{8,8,8,1,1,1}^{u2}$ with average of features + SVM	10

textures in the facial regions using LBP-TOP features that provide an efficient and compact representation for face liveness description. However, very dissimilar strategies were introduced for exploring the temporal dimension even though the same features were utilized. Furthermore, the experiments were carried out using different face normalization techniques and different databases. In this article, we consolidated the methods proposed in the previous studies, isolating the different variables and studying the potential of the different LBP-TOP countermeasures in different settings on the two publicly available datasets. Furthermore, we also provided an open-source framework that makes our research fully reproducible with minimal effort.

Experiments carried out with a unified experimental setup and evaluation methodology showed that the dynamic texture based countermeasure was able to consistently outperform prior work on both datasets. Best results were achieved using nonlinear SVM classifier but it is important to notice that experiments with simpler LDA based classification scheme resulted in comparable performance under various spoofing attack scenarios. Thus, the use of simple and computationally efficient classifiers should be indeed considered when constructing real-world anti-spoofing solutions. In future work, we will study the generalization capabilities of the proposed countermeasure using multiple face anti-spoofing databases. In other words, we plan to perform cross-database experiments by training and tuning the LBP-TOP based face description solely on one dataset and test on another one.

Chapter 5

The Comparative Study

TEXTO INTRODUTORIO

5.1 Databases Permeability

SERAH QUE DEVO FAZER?

5.2 Evaluation Protocol

Firstly, we study how the countermeasures, presented in Section ??, will perform in a more realistic condition. This condition consists in training and tuning each one of the countermeasures with one face anti-spoofing database and testing with another one. To report the performance in such a scenario, two evaluation protocols were designed to work with the databases described in Section 3.3.2. These protocols are the "intra-test" protocol and the "inter-test" protocol.

5.2.1 Intra Database Test Protocol

The intra-test protocol is equivalent to the database normal protocol. It consists in training, tuning and testing a countermeasure with the respectively training set, development set and test set of such a database. With this protocol, it is possible to evaluate the performance and the generalization power of a countermeasure within one database.

5.2.2 Inter Database Test Protocol

The inter-test protocol evaluates the countermeasure performance in a more realistic scenario, close to real usage conditions. It consists in training and tuning a countermeasure with the training set and development set of one database and test it with the test set of another one. With this protocol, it is possible to evaluate the performance and the generalization power of a countermeasure in a set of unseen types of attacks.

5.2.3 Evaluation Metrics

The Replay Attack Database provides a protocol for objective evaluation of a given countermeasure. To mitigate overfitting, such a protocol defines three non-overlapping partitions: the training, development and test set. The training set should be used to train the countermeasure, the development set is used to tune the countermeasure. The test set must be used only to report results.

The CASIA FASD lacks a specific development set; this database has only a train and a test set. To mitigate the over-fitting in this database, the train set was split into five partitions and a 5-fold cross-validation training was done. For that, 4 folds were used for training and 1 fold was used to tune the countermeasure. With this strategy, both databases have a train set, a development set (to tune the countermeasure) and a test set, so it is possible to merge them.

The performance of each countermeasure, using the test set of each database, is reported with the Half Total Error Rate (*HTER*):

$$HTER(D_2) = \frac{FAR(\tau(D_1), D_2) + FRR(\tau(D_1), D_2)}{2}, \quad (5.1)$$

where $\tau(D_n)$ is a threshold, D_n is the dataset, *FAR* is the False Acceptance Rate in the database D_2 and *FRR* is the False Rejection Rate in the database D_2 . In this protocol, the value of $\tau(D_n)$ is estimated on the Equal Error Rate (EER) using the development set of the database D_1 . In this Equation when $D_1 = D_2$, we have the intra-test protocol and when $D_1 \neq D_2$, we have the inter-test protocol.

Because of 5-fold cross validation protocol, for the CASIA FASD 5 results were generated. The average of *HTER* was provided as a final result.

In order to eliminate the face detector influence, the same face detector, based on Modified Census Transform (MCT) features (Froba & Ernst 2004), was used for both databases.

ROC CURVES

Chapter 6

Experiments and Results

This chapter provides the experiments results of this comparative study of countermeasures. Three countermeasures were selected for this study:

- Dynamic textures with $LBP - TOP$;
- Textures with LBP ((Chingovska et al. 2012) and (Maatta and et al. 2012));
- Motion correlation ((Anjos & Marcel 2011)).

As the Motion correlation and $LBP - TOP$ countermeasures need a frame sequence to work, the databases evaluated in this work were the Replay Attack Database (Section 3.3.2) and CASIA Face Antispoofing Database (Section 3.3.3).

The Section 6.2 compare the countermeasures in the Intra-test protocol. Section ?? compare the countermeasures in the Inter-test protocol. In the Section 6.3 the combination of databases is explored to train each one of the countermeasures. In Section 6.4 the Score Level Fusion based Framework is explored to train each countermeasure. Finally Section ?? summarizes the experiments.

6.1 Intra-test protocol

Table 6.1 shows the performance of the three countermeasures, in HTER terms, applying the Intra-test protocol.

Analyzing the performance in the intra-test protocol ($D_1 = D_2$) it can be observed that different countermeasures have different performances in different databases. However, it is possible to observe a that all the three countermeasures have a good overall performance and a good intra-database generalization power. The good generalization performance can be attested comparing the results between the development set and the test set. In Table 6.1 the $HTER(\%)$ in the development set and the $HTER(\%)$ in the test set are very similar. In Figure 6.2 the ROC curves blue and red (dashed line and solid line) represents the intra-test test protocol. It can be observed that the curves are almost overlapped.

Table 6.1: $HTER(\%)$ of each countermeasure applying the intra-test ($D_1 = D_2$) protocol.

Countermeasure	Train/Tune D_1	Test D_2	$HTER(\%)$	
			dev	test
Correlation	Replay CASIA	Replay CASIA	11.66	11.79
$LBPTOP^{u2}_{8,8,8,1,1,1}$	Replay CASIA	Replay CASIA	8.17	8.51
$LBP^{u2}_{8,1}$	Replay CASIA	Replay CASIA	21.77	22.27
			14.41	15.45
			23.00	22.54

6.2 Inter-test protocol

Table 6.2 shows the performance of the three countermeasures, in $HTER$ terms, applying the Inter-test protocol.

Table 6.2: $HTER(\%)$ of each countermeasure applying the inter-test ($D_1 \neq D_2$) protocol.

Countermeasure	Train/Tune D_1	Test D_2	$HTER(\%)$	
			dev	test
Correlation	Replay CASIA	CASIA Replay	11.66	61.78
$LBPTOP^{u2}_{8,8,8,1,1,1}$	Replay CASIA	CASIA Replay	8.17	51.05
$LBP^{u2}_{8,1}$	Replay CASIA	CASIA Replay	21.77	61.11
			46.87	48.06
			23.00	57.64

Analyzing the performance in the inter-test protocol ($D_1 \neq D_2$), it can be observed that the performance results considerably degrade compared with the intra-test protocol and it becomes evident that both databases and the methods are strongly biased indicating the countermeasures do not generalize as expected. In Table 6.2 the $HTER(\%)$ in the development set and the $HTER(\%)$ in the test set are quite different. In Figure 6.2 the ROC curves blue and green (dotted line and solid line) represents the inter-test test protocol. It can be observed that the curves are quite distant from each other.

The results indicate that the countermeasures and the databases introduce some bias on the spoofing detections. The countermeasures bias are possibly related to the feature selection. The databases bias are possibly related with the types and styles of attacks that is hard to generalize. In next experiment, we stray if the countermeasures are truly biased to databases or can be tuned to overcome the database bias.

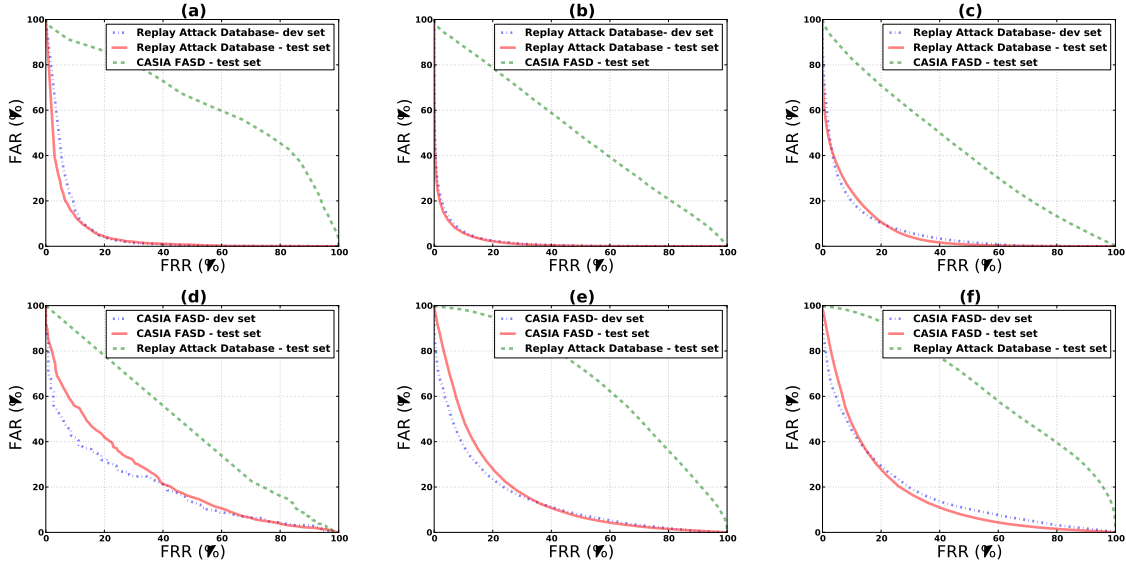


Figure 6.1: ROC curves of each countermeasure using the intra-test and the inter-test protocol. (a) Correlation with frame differences countermeasure trained and tuned with the Replay Attack Database (b) $LBP - TOP$ countermeasure trained and tuned with the Replay Attack Database (c) LBP countermeasure trained and tuned with the Replay Attack Database (d) Correlation with frame differences countermeasure trained and tuned with the CASIA-FASD (e) $LBP - TOP$ countermeasure trained and tuned with the CASIA-FASD (f) LBP countermeasure trained and tuned with the CASIA-FASD.

6.3 Combination of Multiple Databases

Say something.

6.4 Score Level Fusion based Framework

To improve the performance results in comparison with the intra-test protocol and the inter-test protocol and to mitigate the bias mentioned in the last section, we introduce a framework based on score level fusion. Using this framework, when a new countermeasure need to be added, it is possible to "plug it" without any extra training steps required for the other countermeasures.

To support this assumption, we first evaluate the level of independence of the countermeasures trained with different databases in order to ensure its effectiveness in a possible score fusion. Kulcheva and Whitaker (Kulcheva & Whitaker 2003) show that the combination of statistically independent classifiers is a recommended for a good performance in a score level fusion. In order to evaluate the dependence of classifiers, ten statistics were analyzed. The methodology presented on that work shows that the $Q - statistic$ is most suitable and we choose that metric to evaluate the statistic dependence of each countermeasure for the Score Level Fusion based Framework. The $Q - statistic$ for two classifiers is defined as follow:

$$Q_{R,C} = \frac{N_{11}N_{00} - N_{01}N_{10}}{N_{11}N_{00} + N_{01}N_{10}} \quad (6.1)$$

Table 6.3: $HTER(\%)$ of each countermeasure trained with Replay Attack Database and CASIA FASD and test it with each test set of each database.

Countermeasure	Test	$HTER(\%)$	
		dev	test
Correlation	Replay CASIA	12.18	24.14 43.30
$LBPTOP_{8,8,8,1,1,1}^{u2}$	Replay CASIA	14.29	10.67 42.04
$LBP_{8,1}^{u2}$	Replay CASIA	20.45	19.07 45.92

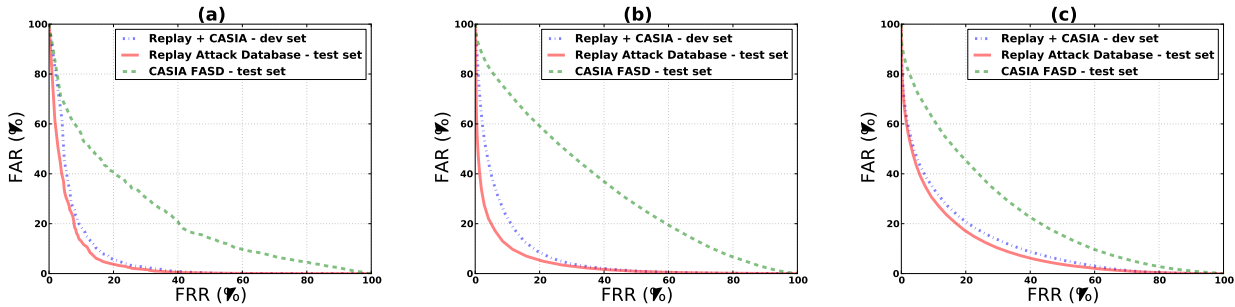


Figure 6.2: ROC curves of each countermeasure trained with Replay Attack Database and CASIA FASD and test it with each test set of each database. (a) Correlation with frame differences (b) $LBP - TOP$ countermeasure (c) LBP countermeasure

where R is the countermeasure trained with the Replay Attack Database; C is the countermeasure trained with CASIA FASD; N_{11} is the number of times that the countermeasure trained with the Replay Attack Database hits (i.e. correctly classifies a sample) and the countermeasure trained with the CASIA FASD also hits; N_{10} is the number of times that the countermeasure trained with the Replay Attack Database hits and the countermeasure trained with the CASIA FASD misses; N_{01} is the number of times that the countermeasure trained with the Replay Attack Database misses and the countermeasure trained with the CASIA FASD hits and N_{00} is the number of times that the countermeasure trained with the Replay Attack Database misses and the countermeasure trained with the CASIA FASD also misses. The range of this measure goes from -1 to 1.

For statistically independent countermeasures it is expected a $Q_{R,C}$ close to 0. Results close 1 means that both countermeasures are very similar and there is no improvement in the fusion. Results close -1 indicates that both countermeasures oppose each other and a high degradation in the fusion should be expected.

Table 6.4 shows the statistic dependency using the $Q - statistic$ and the performance in each database trained with the Score Level Fusion based Framework.

Analyzing the $Q - statistic$ it is possible to observe that the Correlation with Frame Dif-

Table 6.4: $Q - \text{statistic}$ and $\text{HTER}(\%)$ of each countermeasure trained with the Score Level Fusion based Framework and test it with each database.

Countermeasure	Test	$Q_{R,C}$	$\text{HTER}(\%)$	
			dev	test
Correlation	Replay	0.11	13.71	12.39
	CASIA	-0.14		32.08
$LBP TOP^{u2}_{8,8,8,1,1,1}$	Replay	0.24	23.16	26.04
	CASIA	-0.41		38.18
$LBP^{u2}_{8,1}$	Replay	0.38	19.69	21.66
	CASIA	-0.41		47.16

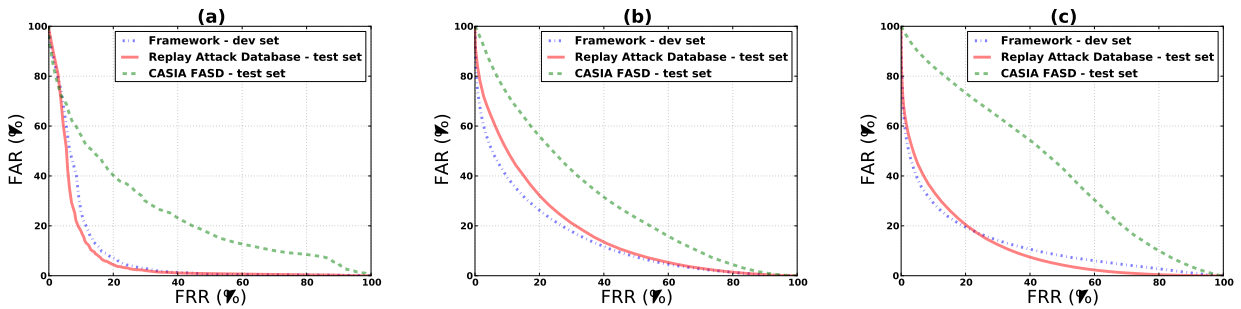


Figure 6.3: ROC curves of each countermeasure trained with the Score Level Fusion based Framework (a) Correlation with frame differences (b) $LBP - TOP$ countermeasure (c) LBP countermeasure.

ferences countermeasure is the most statistically independent and suggests that a score fusion is suitable. This can be attested analysing its performance compared with the inter-test and intra-test protocol results (see Table ??). For the inter-test protocol the improvement with the Score Level Fusion based Framework was significative ($\sim 61.2\%$ in HTER average improvement). Comparing with the intra-test protocol the degradation was very low ($\sim 3.6\%$ in HTER average) and the countermeasure is able to detect spoofs in both databases with different degrees of sucess.

However the $Q - \text{statistic}$ for the $LBP - TOP$ and the LBP countermeasures present unbalanced values for each database. Specially for the CASIA FASD $Q_{R,C} \simeq -0.4$ suggesting that each one of this two countermeasure trained with different databases oppose each other and are not suitable for the Score Level Fusion based Framework. This can be attested analysing their performances compared with the intra-test protocol results (see Table ??). The degradation is still high ($\sim 106.7\%$ in $\text{HTER}(\%)$ average).

The authors that designed the LBP and $LBP - TOP$ countermeasures chosen the SVM with the RBF kernel as classifier. In both settings, the final trained machines have $\sim 35\%$ of the training data as support vectors, what suggest overfitting in each database. The authors that designed the Correlation with Frame Differences countermeasure chosen MLPs with only

5 neurons, which is much simpler classifier and has less chance to overfit of the training data than a SVM.

It is important to remark that the literature lacks in video face spoofing databases and is not possible to ensure the effectiveness of the Score Level Fusion based Framework in a third database. Its effectiveness in a third video face spoofing database, at this stage is only speculative. Another point to highlight is that the fusion strategy chosen for this work is quite simple. For a future extensions more complex fusion strategies need to be addressed.

Chapter **7**

Conclusion

Chapter 8

Future Work

Appendix **A**

Related Publications

Bibliografia

- Anjos, A. & Marcel, S. (2011). Counter-measures to photo attacks in face recognition: a public database and a baseline, *International Joint Conference on Biometrics 2011*.
- Chakka, M., Anjos, A., Marcel, S. & Tronci, R. (2011). Competition on counter measures to 2-d facial spoofing attacks, *Proceedings of IAPR IEEE International Joint Conference on Biometrics (IJCB), Washington DC, USA*.
- Chetty, G. & Wagner, M. (2004). Liveness verification in audio-video speaker authentication, *Proceeding of International Conference on Spoken Language Processing ICMLP*, Vol. 4, pp. 2509–2512.
- Chingovska, I., Anjos, A. & Marcel, S. (2012). On the effectiveness of local binary patterns in face anti-spoofing, *IEEE BIOSIG 2012*.
- da Silva Pinto, A., Pedrini, H., Schwartz, W. & Rocha, A. (n.d.). Video-based face spoofing detection through visual rhythm analysis.
- Duc, N. M., M. B. Q. (2009). Your face is not your password, *Black Hat conference*.
- Eveno, N. & Besacier, L. (2005). A speaker independent” liveness” test for audio-visual biometrics, *Ninth European Conference on Speech Communication and Technology*.
- Flynn, P., Jain, A. & Ross, A. (2008). *Handbook of biometrics*, Springer.
- Froba, B. & Ernst, A. (2004). Face detection with the modified census transform, *Automatic Face and Gesture Recognition, 2004. Proceedings. Sixth IEEE International Conference on*, IEEE, pp. 91–96.
- Galbally, J., Ortiz-Lopez, J., Fierrez, J. & Ortega-Garcia, J. (2012). Iris liveness detection based on quality related features, *Biometrics (ICB), 2012 5th IAPR International Conference on*, pp. 271–276.
- Hill, C. J. (2001). Risk of masquerade arising from the storage of biometrics, *Bachelor of Science thesis, The Department of Computer Science, Australian National University* .

- Jain, A., Bolle, R. & Pankanti, S. (1999). *Biometrics: personal identification in networked society*, kluwer academic publishers.
- Kollreider, K., Fronthaler, H. & Bigun, J. (2009). Non-intrusive liveness detection by face images, *Image and Vision Computing* **27**(3): 233–244.
- Komulainen, J., H. A. P. M. (2012). Face spoofing detection using dynamic texture, *International Workshop on Computer Vision With Local Binary Pattern Variants - ACCV*.
- Kuncheva, L. I. & Whitaker, C. J. (2003). Measures of diversity in classifier ensembles and their relationship with the ensemble accuracy, *Mach. Learn.* **51**(2): 181–207.
URL: <http://dx.doi.org/10.1023/A:1022859003006>
- Leyden, J. (2002). Gummi bears defeat fingerprint sensors, *The Register* **16**.
- Li, J., Wang, Y., Tan, T. & Jain, A. (2004). Live face detection based on the analysis of fourier spectra, *Biometric Technology for Human Identification* **5404**: 296–303.
- Li, S. & Jain, A. (2011). *Handbook of face recognition*, Springer.
- Maatta and, J., Hadid, A. & Pietikaandinen, M. (2012). Face spoofing detection from single images using texture and local shape analysis, *Biometrics, IET* **1**(1): 3 –10.
- Maltoni, D., Maio, D., Jain, A. & Prabhakar, S. (2009). *Handbook of fingerprint recognition*, Springer.
- Martinez-Diaz, M., Fierrez-Aguilar, J., Alonso-Fernandez, F., Ortega-Garcia, J. & Siguenza, J. (2006). Hill-climbing and brute-force attacks on biometric systems: A case study in match-on-card fingerprint verification, *Carnahan Conferences Security Technology, Proceedings 2006 40th Annual IEEE International*, pp. 151–159.
- Matsumoto, T., Matsumoto, H., Yamada, K. & Hoshino, S. (2002). Impact of artificial gummy fingers on fingerprint systems, *Proceedings of SPIE*, Vol. 4677, pp. 275–289.
- Pan, G., Sun, L., Wu, Z. & Lao, S. (2007). Eyeblink-based anti-spoofing in face recognition from a generic webcam, *Computer Vision, 2007. ICCV 2007. IEEE 11th International Conference on Computer Vision*, IEEE, pp. 1–8.
- Tan, X., Li, Y., Liu, J. & Jiang, L. (2010). Face liveness detection from a single image with sparse low rank bilinear discriminative model, *Computer Vision-ECCV 2010* pp. 504–517.
- Wei, Z., Qiu, X., Sun, Z. & Tan, T. (2008). Counterfeit iris detection based on texture analysis, *Pattern Recognition, 2008. ICPR 2008. 19th International Conference on*, pp. 1–4.
- Xiao, Q. (2005). Security issues in biometric authentication, *Information Assurance Workshop, 2005. IAW'05. Proceedings from the Sixth Annual IEEE SMC*, IEEE, pp. 8–13.

- Zhang, H., Low, C., Smolar, S. & Wu, J. (1995). Video parsing, retrieval and browsing: an integrated and content-based solution, *Proceedings of the third ACM international conference on Multimedia*, ACM, pp. 15–24.
- Zhang, Z., Yan, J., Liu, S., Lei, Z., Yi, D. & Li, S. (2012). A face antispoofing database with diverse attacks, *Biometrics (ICB), 2012 5th IAPR International Conference on Biometrics*, IEEE, pp. 26–31.
- Zhao, G. & Pietikainen, M. (2007). Dynamic texture recognition using local binary patterns with an application to facial expressions, *Pattern Analysis and Machine Intelligence, IEEE Transactions on* **29**(6): 915 –928.
- Zhu, Q., Chatlani, N. & Soraghan, J. (2012). 1-d local binary patterns based vad used inhmm-based improved speech recognition, *Signal Processing Conference (EUSIPCO), 2012 Proceedings of the 20th European*, pp. 1633–1637.